Earth Reinforcement, Ochiai, Yasufuku & Omine (eds) © 1997 Balkema, Rotterdam, ISBN 90 5410 833 9

Performance of reinforced soil structures during the 1995 Hyogo-ken Nanbu Earthquake

F.Tatsuoka
University of Tokyo, Japan

J.Koseki
Institute of Industrial Science, University of Tokyo, Japan

M.Tateyama
Railway Technical Research Institute, Japan

ABSTRACT: The performance of a number of mechanically stabilized earth retaining walls and nailed slopes during the 1995 Hyogo-ken Nanbu earthquake is reviewed. The behaviour of the reinforced soil retaining walls is compared with that of the conventional retaining walls. Some lessons from the case histories and limitations of the current seismic design methods are discussed. Reconstruction of damaged structures by soil reinforcing techniques is also presented.

1 INTRODUCTION

This paper will discuss the seismic stability of reinforced soil structures, including reinforced sloped embankments, soil retaining walls and natural slopes. This topic has always been a major concern of geotechnical engineers in high seismicity regions including Japan. The major issues may include:
a) stability for seismic loads relative to the stability for static loads;
b) seismic stability relative to other types of civil engineering structures (e.g., elevated RC frame structures); and
c) relative seismic stability among different types of soil structures (e.g., unreinforced versus reinforced soil structures).

Issue a) is related to the aseismic design methodologies for soil structures. Compared with ordinary steel and RC structures, soil structures in secondary applications are usually not aseismic-designed. Important soil structures are usually aseismic-designed, but they are by the limit equilibrium-based pseudo-static method using a relatively a low seismic coefficient k_h such as 0.20. Probably, this situation results from such a consideration that in case soil structures in secondary applications are damaged, the influence of the damage would not be vast and serious and they could be easily repaired. Also, the use of higher k_h values could result in higher construction cost. However, to be consistent with the recent trend of aseismic design methodologies for steel and RC structures which employ much higher seismic loads than before, we need rationales for the above-mentioned conventional aseismic design methodologies or new aseismic design methodologies for soil structures including reinforced soil structures.

For "reinforced soil retaining walls (RWs) to retain embankment (Fig. 1d)", for example, Issues b)

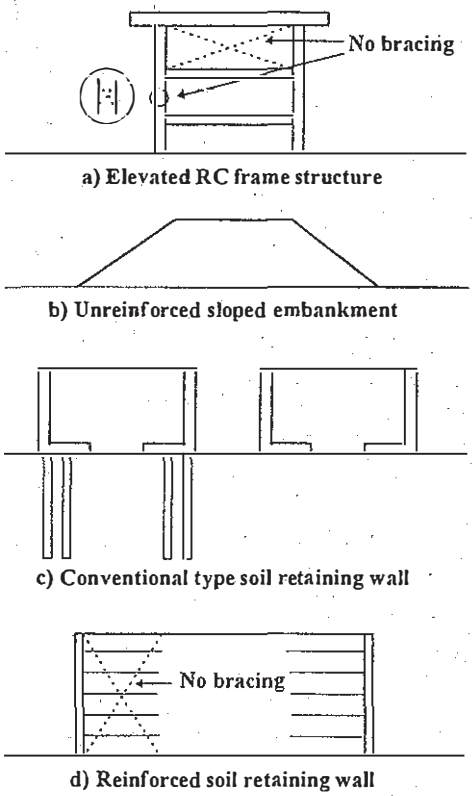

Fig. 1 Schematic figures of a) elevated RC frame structures, b) sloped embankment, c) RC RWs, and d) Reinforced soil RWs.

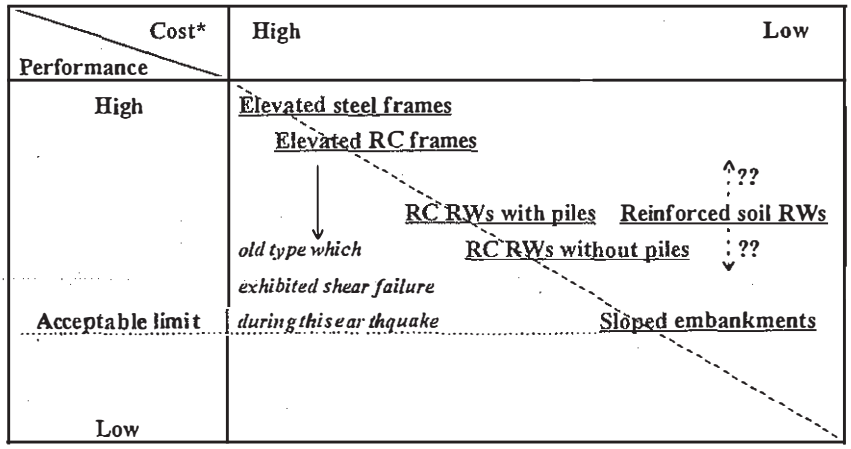

* at the time of construction

Fig. 2 Approximated relative cost and performance of typical different types of elevated structures

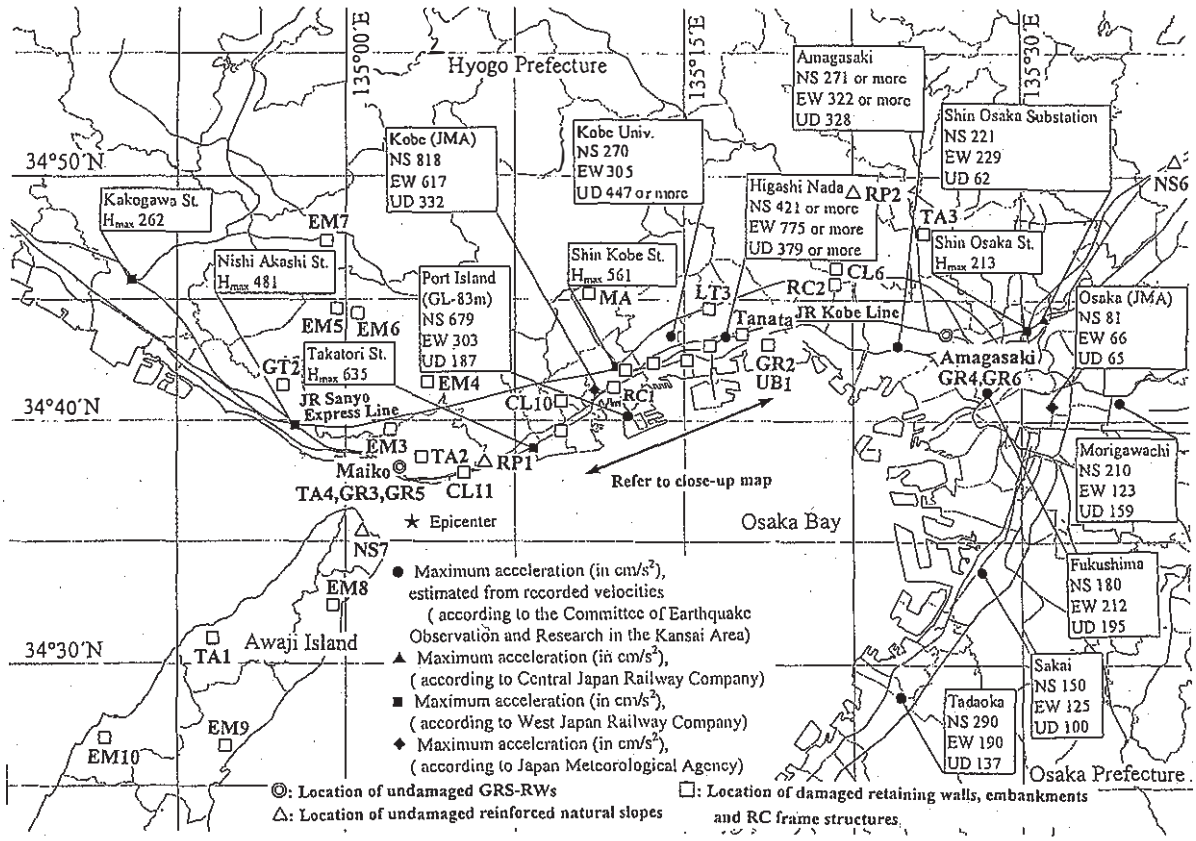

Fig. 3 Recorded peak ground acceleration and locations of typical structures described in the paper.

and c) are linked to their advantages over unreinforced sloped embankments (Fig. 1b), conventional type soil RWs (Fig. 1c), and elevated RC frame structures (Fig. 1a). It is common to try to select a structure type which is the most cost-effective while satisfying the required level of performance. In Fig. 2, the structures having the same cost-effectiveness are located at the same distance from the diagonal line extending from the top left corner to the bottom right corner. Reinforced soil RWs are usually more cost-effective than the conventional soil RWs, located more toward the top right corner. Even when a higher cost-effectiveness is assured, however, it is not certain whether or not the performance (i.e., seismic stability in this case) of a given reinforced soil structure could be equivalent to, or higher than, that of the conventional structures (e.g., conventional type RC RWs and elevated RC frame structures).

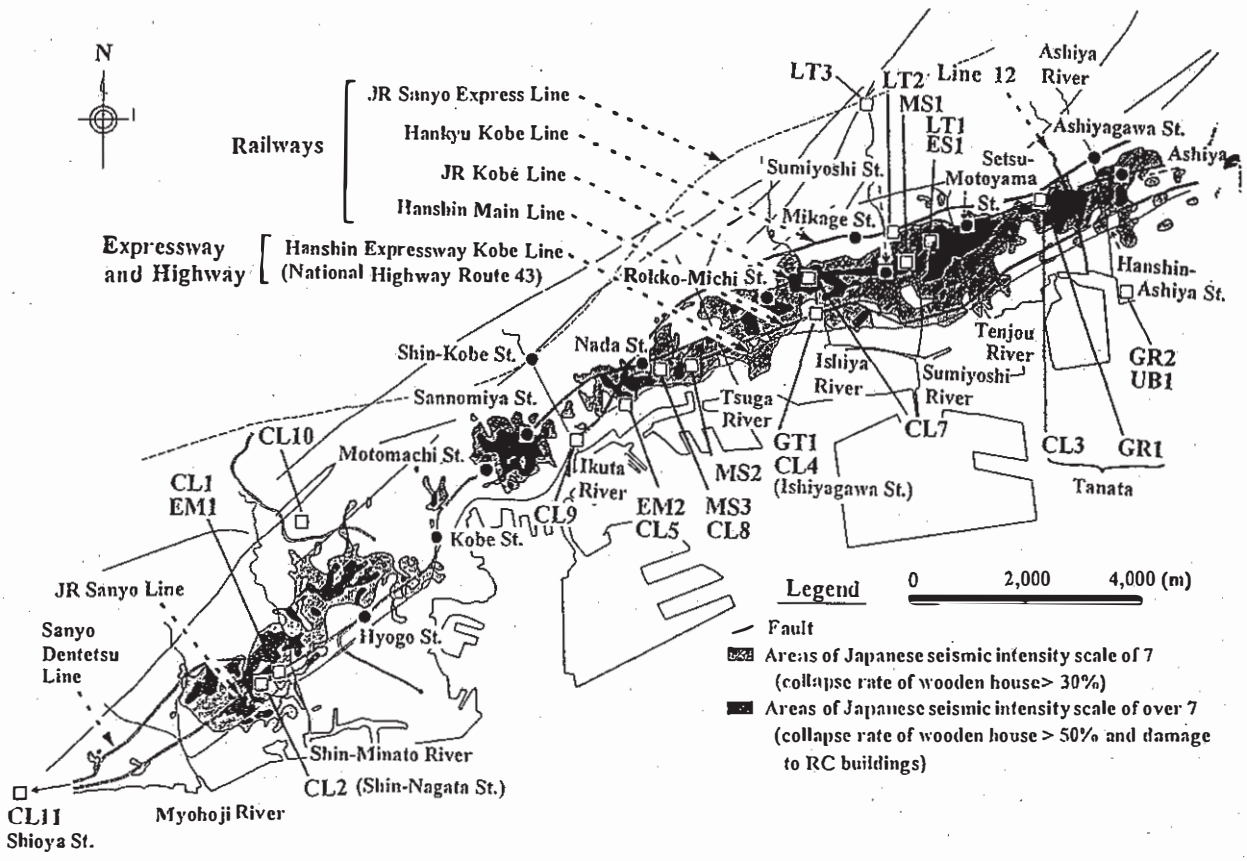

Fig.4 Areas of JMA scale equal to seventh or higher and locations of typical structures described in the paper.

Varying degrees of damage to a great number of various type old and recent civil engineering structures caused by the 1995 Hyogo-ken Nanbu earthquake provided us a great opportunity to examine the above issues. It will be attempted to review the performance of reinforced soil structures, as much as possible, in view of the points described above.

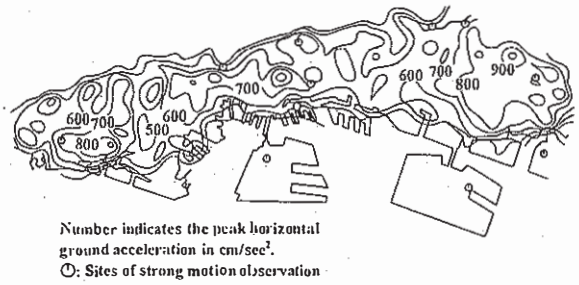

Fig. 5 Estimated contours of PHGA (after Fig. 13 of Sato, 1996).

2 OVERVIEW OF THE EARTHQUAKE AND DAMAGE TO CIVIL ENGINEERING STRUCTURES

2.1 *The Earthquake*

At 5:46 a.m. 17th January 1995, a devastating earthquake measuring 7.2 on the Richter scale hit the southern part (i.e., "nanbu" in Japanese) of Hyogo Prefecture, including Kobe City. The representative recorded peak horizontal ground accelerations (PHGAs) and vertical ones are shown in Fig.3. Fig.4 shows the areas where the Japanese Meteorological Agency seismic intensity scale (JMA scale) was seventh or higher, estimated from the collapse ratio of wooden houses (Chuo Kaihatsu Corp., 1995), which is consistent with the distri-bution of PHGA estimated by Sato (1996) (see Fig. 5).

Fig. 6 shows the response spectrum curves for a damping ratio equal to 5 % for the ground horizontal acceleration recorded at Kobe (JMA) and others (see Fig. 3). The predominant period was around 0.3 - 1.0 seconds. This and other similar records suggest that structures having natural period of around 0.3 - 0.5 seconds while having low damping properties should have proven to be most seriously damaged,

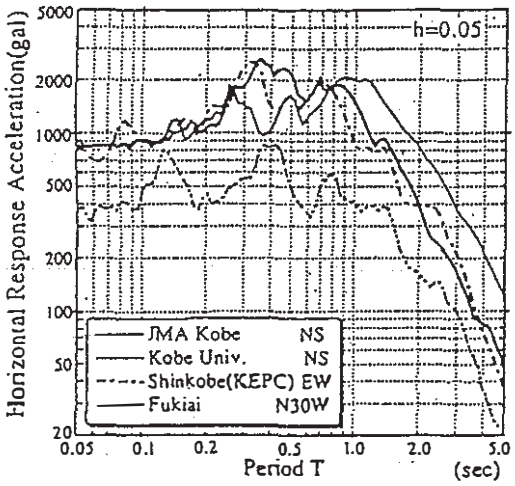

Fig. 6 Response spectrum curves of some typical recorded earthquake records (after Fig. 3 of Sato, 1996)

because the response could be large at the initial stage of loading and it could not decrease much with the increase in the natural period T_n although the damping increased as the damage became more severe.

2.2 *Damage to civil engineering structures*

Perhaps one of the best case histories to examine relative seismic stability of typical civil engineering structures is the performance of elevated RC frame structures, embankment slopes and conventional type soil RWs constructed for and adjacent to the JR Kobe and Sanyo Lines located in the affected areas (see Figs. 3 and 4 for the locations). The performance of reinforced soil structures will be reviewed later. The railway was extended from Osaka to Kobe by 1874, constructed mainly on the ground surface, partly on embankments with vertical:horizontal slopes of 1:1.5. The railway was extended to the west of Kobe Station as the Sanyo Line from 1894.

Elevated RC frame structures: For grade separation in the urban area, with a length of about 0.74 km between San-no-miya and Motomachi Stations (see Fig. 4), elevated RC frame structures were constructed by 1938. They were 8-9 m high on average. It is considered that the design was rather conservative as evident from a relatively short center-to-center spacing of 5.5 m between RC columns in the longitudinal direction. A large number of RC columns were damaged, but none of them totally collapsed, and after necessary repair, the railway was reopened only 34 days after the earthquake.

After World War II, the railway for a length of about 3.3 Km between Sumiyoshi and Nada Stations (see Fig. 4) on the ground surface and embankments was reconstructed by 1976 on elevated RC frame structures, including RC bridge girders and their RC frame abutments. Based on the design code specified in 1970, the design was more economical than before, as seen from a wider center-to-center spacing of 8 m between RC columns. Many of the columns were much more seriously damaged and some totally collapsed mainly due to shear failure as typically seen from Figs. 7a and b. Seventy one columns, which were nearly a half of the total columns, were reconstructed. The undamaged columus were only 20 % of the total columns (RTRI, 1996). The railway was reopened on 1st April 1995, 74 days after the earthquake.

The likely reasons for such serious damage to the RC columns are as follows:

1) Also outside the areas where Japanese wooden houses were seriously damaged (as shown in Fig. 4), a large number of RC columns were seriously damaged. Typically, about 30 columns of the elevated RC frame structures for the Bullet Train Line (Shin-kansen) located north of Ashiya (RC2; see Fig. 3) were totally collapsed and reconstructed. The behaviour of the elevated RC frame structures of the Kobe Line and the Bullet Train Line would be due partly to highly amplified responses, caused by the following two factors; i) most of the damaged elevated RC frame structures had predominant period T_n about 0.5-0.8 second, and ii) the RC columns had low damping ratios when compared with soil structures, which exhibited high damping ratios when undergoing large deformation before reaching ultimate failure.

2) The elevated RC frame structures had no overall bracing and no diagonal steel reinforcement in each column (Fig. 1a). They were, therefore, basically not well prepared for large tensile loads acting in the diagonal direction caused by lateral seismic loads. The damaged RC columns were prone to shear failure, mainly due to over-estimation of the shear strength of concrete in the design and an insufficient amount of stirrups. Shear failure of RC columns occurs in a rather brittle manner, easily resulting in total collapse. Recent RC columns are, therefore, designed not to fail by shear failure but by bending failure, based on the design code specified in 1983. Note that many of the independent RC piers supporting steel or RC girders for elevated highways located inside and outside the most severely shaken areas were also seriously damaged, mainly by shear failure, and some of them were totally collapsed.

Reinforced soil RWs are reinforced with horizontal reinforcement with or without a vertical full-height rigid facing, while no inextensible members are

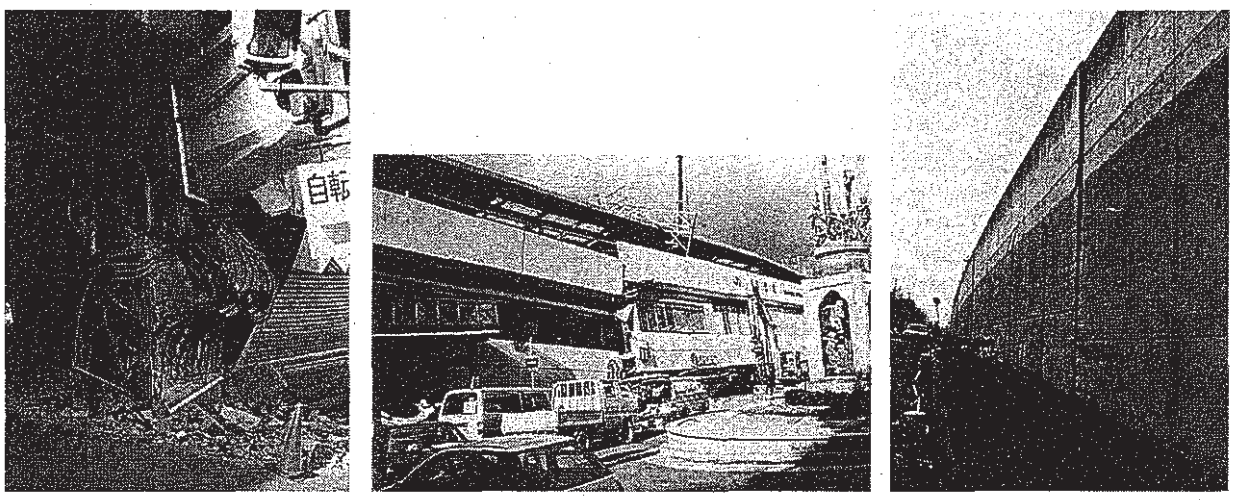

a) b) d)

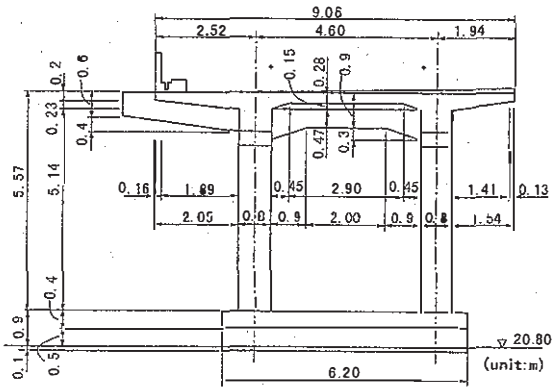

c)

Fig. 7 a) Damaged RC frame bridge abutment and b) damaged Rokko-michi Station consisting of elevated RC frame structures, c) typical dimensions of elevated RC frame structure, and d) inverted T-shaped RC RW adjacent to Rokko-michi Station.

ranged in the diagonal direction where tensile strains become the largest (Fig. 1d). This feature is similar to that of elevated RC frame structures. This point will be discussed later.

Soil structures: Many of the sloped embankments constructed for grade separation of the JR Kobe and Sanyo Lines suffered from large settlement and lateral movement, accompanied by longitudinal tensile cracks on the top near the slope and along the slope surface, resulting in large settlement and lateral movement of the railway tracks. At some locations, the toes of slopes were supported by low gravity type RWs, which were 1.0 - 1.5 m in the total height with a buried depth of 0.5 m (Fig. 8). Despite their small heights, most of them completely overturned to the ground surface. Most of the slope surface had been covered with a cast-in-place concrete lattice and precast concrete plates to protect the slope against against heavy rainfall, but they were found to be ineffective in preventing the deformation of the embankment due to seismic loads. This damage was induced very likely by the high seismic force applied to the facing itself.

The oldest type of RW is masonry RWs. They were constructed more than 70 years ago without aseismic design. They were most seriously damaged among different types of RWs. Most of the masonry RWs located in the areas where the JMA scale was equal to seventh or higher were more-or-less damaged as typically shown in Fig. 9. Many masonry RWs supporting the backfill behind the RC bridge abutments moved outward, resulting in large settlement of the backfill relative to the pile-supported RC bridge abutments.

For a length of about 600 m between Setsu-motoyama and Sumiyoshi Stations (see Fig. 4), the north side slope of embankment was retained by leaning-type unreinforced concrete soil RWs constructed around 1938. The RWs were either broken at the ground surface level and the upper part overturned completely to the ground surface or overturned about the bottom, resulting in the back face facing up (Fig. 10a). This damage was perhaps triggered by large horizontal seismic loads acting on the RW structure itself and large seismic earth pressure imposed on its back face from the backfill. It seems, however, that the former factor should be the major factor for complete overturning of the RW.

Shin-Nagata Station of the JR Sanyo Line was constructed around 1965 on the crest of a sloped embankment. Both sides was supported by cantilever-type (or inverted T-shaped type) RC RWs for a total length of about 800 m (Fig. 11a). The walls were aseismic-designed using k_h= 0.2, but it is

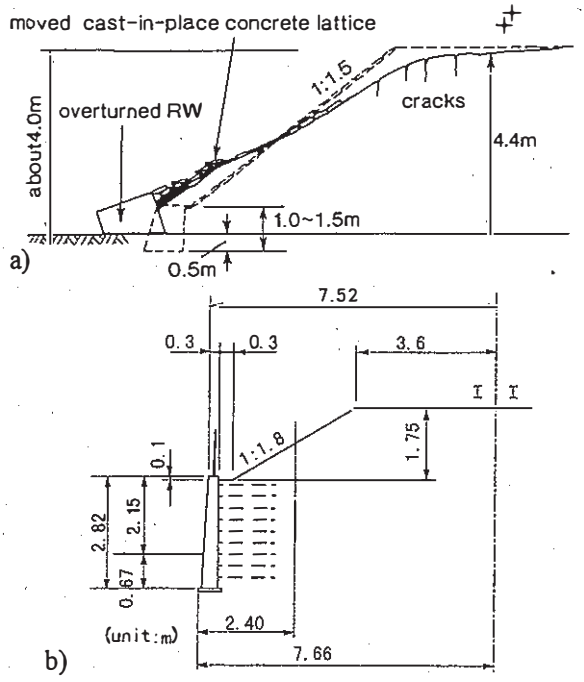

Fig. 8 Cross-sections of a) a typical damaged south slope of the embankment and b) a GRS-RW by reconstruction, between Setsu-motoyama and Sumiyoshi Stations, JR Kobe Line (ES1 in Fig. 4).

very likely that they were not supported by piles despite a weak subsoil. Most of these RWs considerably tilted and slid outward at the bottom inducing large settlement at the top of the railway embankment. It seems that the damage was due to insufficient values of both the bearing capacity in the subsoil beneath the wall and the sliding resistance at the wall base. The most serious damage was cracking in the facing, probably due to extra-ordinary large seismic earth pressure from the sloped backfill (Fig. 11a).

Inverted T-shaped and buttressed RC RWs which was constructed around 1938 at Shioya Station of the Sanyo Dentetsu Line, running in parallel to the JR Sanyo Line (see Fig. 4), were also seriously damaged (Fig. 12, CL11 in Fig. 3). There were no piles. Although the wall did not totally collapse, most part tilted largely for a length of about 360 m, and some part of the wall structure ruptured. Similar to the RWs at Shin-nagata, the strength of the wall structure itself and the bearing capacity of the supporting subsoil below the wall were seemingly not sufficient to prevent, respectively, the failure of the wall structure and the large tilting of the wall. The walls were removed after the earthquake.

The seismic behaviour of a RC RW which was constructed most recently (in 1992) to retain the south face of the embankment for the JR Kobe Line

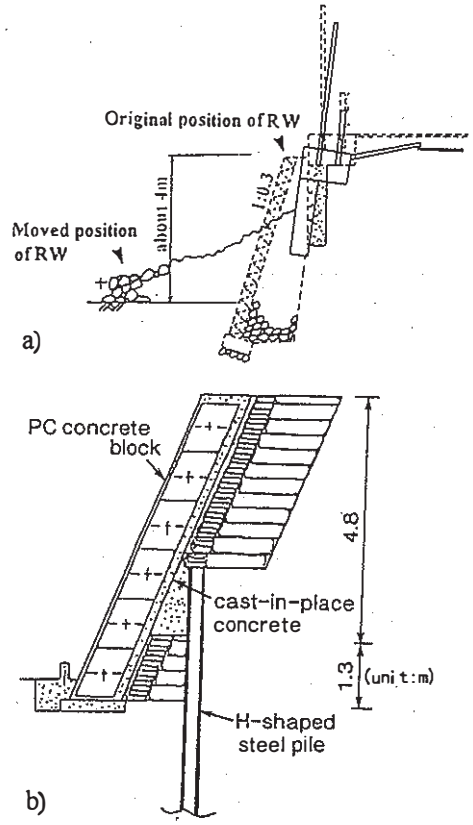

Fig. 9 Cross-sections of a) a typical damaged masonry RW constructed in around 1925 (MS1 in Fig. 4) and b) a GRS-RW by reconstruction (the facing consists of PC concrete blocks, which were fixed afterwards to each other and to the backfill), between Setsu-motoyama and Sumiyoshi Stations, JR Kobe Line.

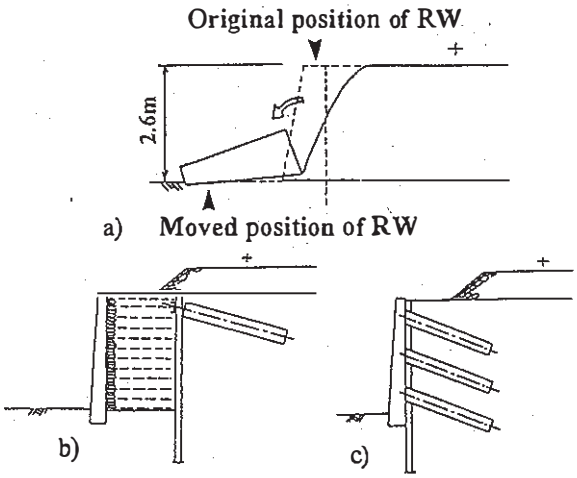

Fig. 10 Cross-sections of a) a typical damaged leaning-type RW constructed in 1937 (LT1 in Fig. 4), and b) a GRS-RW and c) a nailed RW by reconstruction, the north side slope of the embankment between Setsu-motoyama and Sumiyoshi Stations, JR Kobe Line.

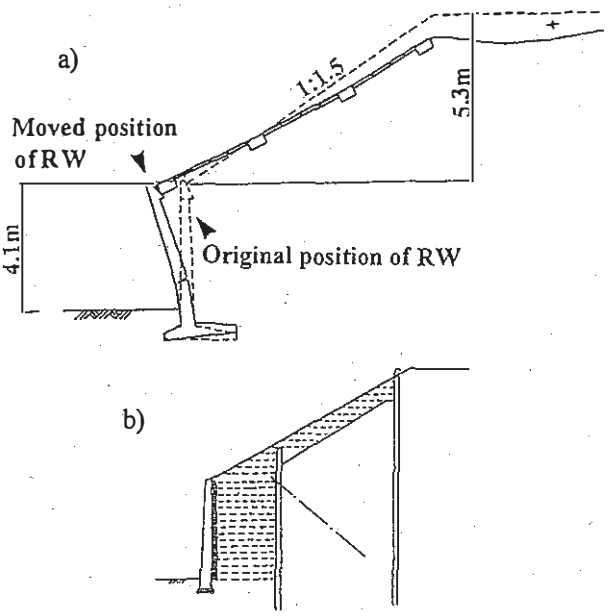

Fig. 11 Cross-sections of a) a typical damaged cantilever-type RC RW without a pile foundation (CL2 in Fig. 4) and b) a GRS-RW by reconstruction, at Shin-nagata Station, JR Sanyo Line.

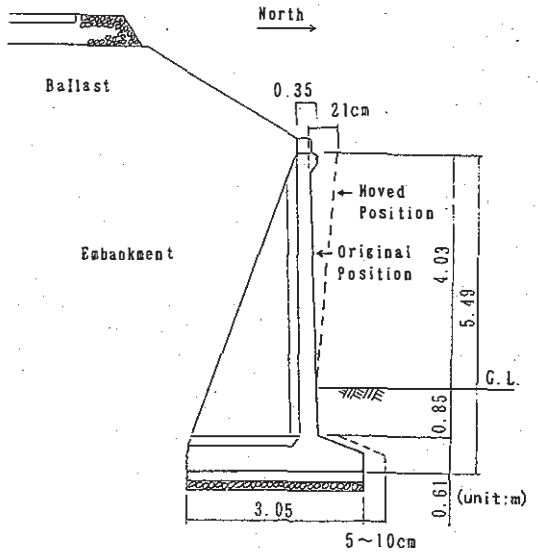

Fig. 12 Typical cross-section of damaged buttressed RC RW without a pile foundation (CL11 in Fig. 4), Shioya Station, Sanyo Dentetsu Line.

at Tanata site (CL3 in Fig. 2) will be discussed later in this paper.

Gravity-type unreinforced concrete RWs is another old type. They were constructed more than 60 years ago. The walls at the Ishiyagawa Station of the Hanshin Line (Fig. 13, GT1 in Fig. 4) were most seriously damaged, although these walls were aseismic-designed by using k_h= 0.2.

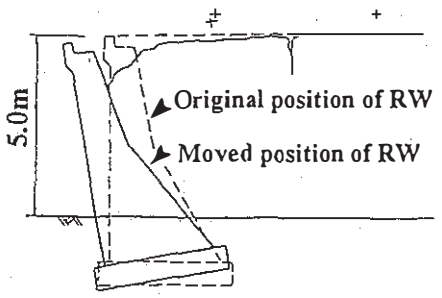

Fig. 13 Cross-section of the seriously damaged gravity type unreinforced concrete RW at Ishiyagawa Station (GT1 in FIg. 4), Hanshin Railway Main Line.

In Tables 1 and 2, damaged embankments and conventional type soil retaining structures constructed for railways and roads, including those described above, are summarized. The features of the damage could be summarized as follows:

1) In contrast to the damaged RC columns and piers, most seriously damaged soil structures were located in the zones where Japanese wooden houses were seriously damaged (Fig. 4). The major reason is perhaps their low amplified responses due to high damping ratios at large strains and presumably the undamaged natural periods T_n that were much shorter than the range of T_P (Fig. 6).

2) A number of embankments and gravity type soil RWs were seriously damaged. Their failure was triggered by i) shear failure within the slope or overturning of the wall induced by high seismic loads applied to the embankments and wall structures, and/or ii) failure in the subsoil. The former cases were observed mostly in the most severely shaken areas. Among the latter cases, catastrophic failure was triggered by soil liquefaction in the sub-soil, which was observed outside the most severely shaken areas shown in Fig. 4 (e.g., RWs; UB1 and GR2 and embankments; EM3 through EM9). A similar type of failure was observed also for a large portion of river dikes.

3) Among the conventional RWs, which are masonry RWs, leaning-type (supported type) unreinforced concrete RWs, gravity-type unreinforced concrete RWs, and cantilever-type or inverted T-shaped type RC RWs (mostly without piles), the first three types of RW were most seriously damaged, and the failure was catastrophic, despite that except for the masonry RWs, they had been aseismic designed. It is likely that even without seismic earth pressure applied to the back face, they would have ruptured or tilted or even completely overturned due to seismic loads exerted on the wall structure itself. A very wide gravity-type unreinforced concrete RW supported by piles would have been stable even during this level of earthquake, but this type of RW is never cost-effective.

4) For many of the damaged RWs, the bearing

Table 1 Damaged retaining walls for railways and roads.

Facility	Site	Location	Type of wall	Height/ length of wall	Subsoil condition	Brief description of damage/ permanent restoration method
Railway	MS1	Between Setsu-Motoyama & Sumiyoshi Stations of JR Kobe Line	Masonry	4 m/ 50 m	-	Total collapse/ GRS-RW
Railway	MS2	Adjacent to Nishi-Nada Station of Hanshin Main Line	Masonry	3.4 to 3.8 m/ 80×2 m	-	Tilting of upper wall, settlement of embankment/ GRS-RW
Road	MS3	City Road Nishi-Nada-Harada and Rokko-Sannomiya Lines at Iwayakita 3 & 4-chome, Nada-ku, Kobe City	Masonry	max. about 5 m/70 m	-	Vertical and horizontal cracking of wall, lateral deformation and settlement of embankment/ ?
Railway	LT1	Between Setsu-Motoyama & Sumiyoshi Stations of JR Kobe Line	Leaning-type	2.6m/500m	Pleistocene gravel (N_{SPT}= 15~50 up)	Complete overturning, partial breakage at the level of subsoil surface/ GRS-RW, RW with embankment reinforced by large diameter nailing
Railway	LT2	Between Okamoto and Mikage Stations of Hankyu Kobe Line	Leaning-type	8.0 m/ 500×2 m	-	Tilting on both sides, cracking near the bottom, settlement of embankment/ U-shaped RW filled with cement-treated soil
Road	LT3	City Road Higashi-Nada-sato No.143 Line at Higashi-Nada-ku, Kobe City	Leaning-type	max. about 5 m/ 160 m	-	Vertical opening and horizontal sliding at constuction joint/ partial reconstruction to increase wall height
Railway	GT1	Adjacent to Ishiyagawa Station of Hanshin Main Line	Gravity-type	5.0 m/ 200×2 m	Holocene sand (N_{SPT}=10~30)	Tilting on both sides, partial breakage at construction joint and overturning/ viaduct
Road	GT2	City Road Ookubo No.18 Line at Ookubo-cho, Akashi City	Gravity-type	max. 3.0 m/ 160 m	-	Tilting, longitudinal cracking of embankment/ reconstruction of original RW
Railway	CL1	Between Hyogo & Shin-Nagata Stations of JR Sanyo Line	Cantilever-type	4.0 m/ 400×2 m	-	Tilting on both sides, settlement of embankment, deformation of footpath/ reinforcement by anchoring and tie-rods
Railway	CL2	At Shin-Nagata Station of JR Sanyo Line	Cantilever-type	4.1 m (+5.3m for overlying embankment)/ 200m	Holocene clay (N_{SPT}= 5)	Tilting and sliding, cracking at the middle height, settlement of embankment/ GRS-RW, cantilever-type RW with pile foundation
Railway	CL3	At Tanata between Ashiya & Setsu-motoyama Stations of JR Kobe Line	Cantilever-type with pile foundation	5.4 m/ 50 m	Holocene sand and clay (N_{SPT}=25~50 & 10~25)	Tilting and sliding, settlement of embankment/ reinforcement by horizontal tie-rods connected to upper RW adjacent to RC box
Railway	CL4	Adjacent to Ishiyagawa Station of Hanshin Main Line	Cantilever- type	5.0m/30m	Holocene sand (N_{SPT}=10~30)	Tilting, cracking at the middle height of a section without counterforts/ viaduct
Railway	CL5	Between Higasbi-Nada & Kobe-kou Stations of JR Kobe Line (freight branch)	Cantilever-type	4.5 m (+1.8 m for overlying embankment)/ 50m	-	Tilting, cracking near the bottom, settlement of embankment/ cut-off sheet piles with tie-rods & outer backfill reinforced by geogrid
Road	CL6	Prefectural Highway Shioze-Mondosou Line at Koma-no-machi, Takarazuka City	Cantilever-type	about 4 m/ 80 m	(Adjoining waterway)	Subsidence, tilting and sliding of wall, longitudinal fissuring of embankment/ reconstruction of original RW
Road	CL7	City Road Yamate Main Line at Yuminoki-1-chome, Nada-ku, Kobe City	Cantilever-type	about 3 m/60 m	-	Tilting of wall, longitudinal fissuring of embankment/ Terre Annee
Road	CL8	City Road Nishi-Nada-Harada and Rokko-Sannomiya Lines at Iwaya-Kita 3 & 4-chome, Nada-ku, Kobe City	Cantilever-type ? (not confirmed)	max. about 5 m/250 m	-	Tilting and vertical cracking of wall, opening of vertical joint, settlement of embankment/ Terre Annee
Road	CL9	Regional Highway Baiko-Hamabedori-Wakihama Line at Masago-dori 1 & 2-chome, Chuo-ku, Kobe City	Cantilever-type ? (not confirmed)	max. 3.7 m/ 310 m	-	Tilting of wall (cracking of side wall of RC box culvert adjoining the wall)/ reconstruction of original RW?
Road	CL10	Regional Highway Sanroku Line at Hiyodorigoe, Hyogo-ku, Kobe City	Cantilever-type ? (not confirmed)	max. 4.5 m/ 40m	Holocene sand (N_{SPT}=3~50)	Sliding of wall/ reinforcement by earth anchor fixed to firm subsoil
Railway	CL11	Shioya Station of Sanyo Dentetsu Line	Cantilever-type	about 4 m/ 360m	-	Tilting of wall/ viaduct
Road	UB1	City Road Ashiya-hama Line at Midori-cho, Ashiya City	U-shaped with inner backfill	about 2 m/ 560m	-	Uneven settlement and tilting/ reconstruction of original RW, correction of wall height
Railway	GR1	At *Tanata* between Ashiya & Setsu-motoyama Stations of JR Kobe Line	GRS with rigid facing	max. 4.5 m/ 300 m	Holocene sand and clay (N_{SPT}=5~50 & 5)	Tilting and sliding, partial cracking of facing at the middle height, settlement of embankment/ reinforcement by horizontal tie-rods connected to upper RW adjacent to RC box
Park	GR2	In Maihama Park at Ashiya-hama, Ashiya City	GRS with concrete-block facing	5.3 m (+1.0 m for overlying embankment)/ 90m	-	Uneven settlement and opening of facing blocks (+extensive sand boil and fissures due to liquefaction at the subsoil surface)/ ?
Road	GR3	Near approach road to Akashi Kaikyo Bridge (under construction) at *Maiko*, Tarumi-ku, Kobe City	GRS with flex. metal-mesh facing	max. 4.0m/ 95 m	-	Slight differential horizontal movement of sound barrier foundation at the top of embankment (uneven settlement & fissures at the subsoil surface)
Railway	GR4	Near *Amagasaki* Station of JR Kobe Line	GRS with rigid facing	max. 8 m (av. 5 m)/ 1000m (including two abutments by GRS-RW)	-	No damage

Table 1 Damaged retaining walls for railways and roads. (continued)

Facility	Site	Location	Type of wall	Height/length of wall	Subsoil condition	Brief description of damage/ pennanent restoration method
Railway	GR5	Near approach road to Akashi Kaikyo Bridge (under construction) at *Maiko*, Tarumi-ku, Kobe City	GRS with rigid facing	max. 6.7 m/ 150 m	-	No damage
Railway	GR6	Near *Amagasaki* Station of JR Kobe Line	GRS with rigid facing	max. 8 m/ 400 m	-	No damage
Road	MA	Kita-Kobe Line of Hanshin Express way at Kami-Tanigami, Yamada-cho, Kita-ku, Kobe City	Mu tiple-anchor-reinforced soil with RC facing	max. 4.6 m/ 24 m	-	Tilting of cap concrete without anchors at the top of RW/ ?
Road	TA1	National Highway Route No.28 at Hokutan-cho, Awaji Island	Terre Annee	max. 8.9 m/ ? m	-	Tilting of facing, partial cracking of facing at the corner/ reconstruction using lengthened metal-strip
Park	TA2	In Hoshi-ga-oka Park at Tarumi-ku, Kobe City	TerreAnnee	max. 5.1 m/ 43 m	-	Tilting and sliding of facing, partial cracking of facing at the corner/ ?
Others	TA3	In Midori-ga-oka Pool at Itami City	TerreAnnee	max. 3.3 m/ 36 m	-	Tilting off acing, partia cracking off acing at the corner, settlement of embankment/ ?
Road	TA4	Approach Road to Akashi Kaikyo Bridge (under construction) at *Maiko*, Tarumi-ku, Kobe City	TerreAnnee	max. 6-7 m/ ? m	-	Noticeably compressing at the bottom of facing / ?

RW: retaining wall, GRS: geogrid-reinforced soil, Terre Armee: metal-strip reinforced soil with discrete RC facing

Table 2 Damaged embankments for railways and roads.

Facility	Site	Location	Slope angle/ facing condition	Height/ length of embankment	Subsoil condition	Brief description of damage/ pennanent restoration method
Railway	EM1	Between Hyogo & Shin-Nagata Stations of JR Sanyo Line	1:1.5/ cast-in-place concrete lattice and precast concrete panel	4.4 m/450 m (full embankment)	-	Settlement and lateral deformation, sliding of concrete facing/ embankment partially reinforced by geogrid and covered with geomembrane (artificia lawn type)
Railway	EM2	Between Higashi-Nada & Kobe-kou Stations of JR Kobe Line (freight branch)	1:1.5/ vegetation	6.0 m/320 m (full embankment)	-	Settlement and lateral deformation, longitudinal crack/ embankment reinforced by large diameter nailing
Road	EM3	Ookura-dani Interchange of the Second Shinmei Expressway	-	15 m/30 m (full embankment)	Soft clay and partial sand (N_{SPT}<5, former pond)	Collapse of embankment/ ?
Road	EM4	Regional Highway Kobe-Kakogawa-Himeji Line at Zenkai, Ikawadani-cho, Nishi-ku, Kobe City	1:2.0/ precast concrete panel	7 m/ ? m (half bank)	(existing pond at slope toe)	Sliding of slope and facing/ reinforcement by sheet pile driven at the middle of slope
Road	EM5	Regional Highway Kobe-Kakogawa-Himeji Line at Minami, Kande-cho, Nishi-ku, Kobe City	-	max. 8 m/ ? m (half bank)	(existing pond at slope toe)	Collapse of embankment/ ?
Road	EM6	Regional Highway Kobe-Kakogawa-Himeji Line at Wada, Oshibedani-cho, Nishi-ku, Kobe City	-	? m/ ? m (half bank)	(existing pond at slope toe)	Sliding of slope/ ?
Road	EM7	City Road Fukui Line at Fukui, Miki City	-	max. 13 m/66 m (full embankment)	(existing pond at slope toe)	Collapse of embankment/ protection work against seepage of water from existing pond?
Road	EM8	Town Road Ura No.105 Line at Kusumoto, Higashiura Town, Tsuna District	-	? m/ 116 m (half bank)	(swamp)	Collapse of embankment/ reconstruction of original embankment
Road	EM9	Town Road Takataki Line at Ikuho, Tsuna Town, TsunaDistrict	-	max. 7.5 m/ 34 m (half bank)	(swamp)	Collapse of embankment/ cast-in-place concrete lattice and partial drainage mat in embankment
Road	EM10	Town Road Hirata-Shitamichi Line at Takayama, Ichinomiya Town, Tsuna District	-	? m/ 30 m (half bank)	-	Collapse of embankment/ reconstruction of original embankment

capacity of the subsoil and shear resistance along the wall base was not enough to prevent the failure by overturning and base sliding. Although the use of a strong pile foundations could have effectively prevented this type of failure, the construction cost would have become high.

5) A number of RC columns and piers were seriously damaged or even totally collapsed. Compared with them, a number of modern RC RWs supported by piles and reinforced soil RWs performed much better.

Brittle versus ductile behaviour: The ductility of a structure means the capability for large energy absorption after yielding, which means a large area between the post-yield load-displacement curve and the horizontal axis (Fig. 14). In this schematic figure, according to concrete engineering, the ductility μ for a given structure is defined as the ratio δ_u / δ_y, where δ_u and δ_y are the deformation at the ultimate failure where the strength drops rapidly to zero or a near-zero residual strength

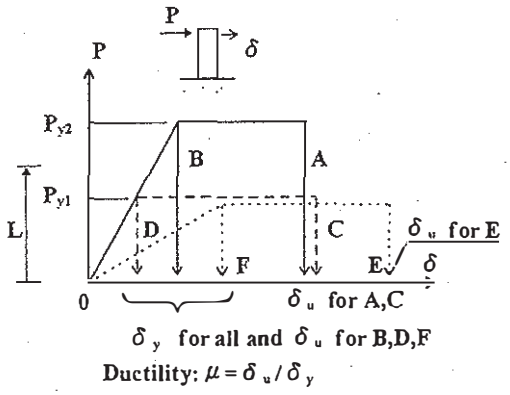

Type	Preyield stiffness	Yield strength	Ductility
A	High	High	High
B	High	High	Low
C	High	Low	High
D	High	Low	Low
E	Low	Low	High
F	Low	Low	Low

Fig. 14 Seismic structure characterization by pre-yield stiffness, yield strength and ductility (a schematic figure).

and the deformation at yielding, respectively.

In Fig. 14, structures A, B, C and D have the same high pre-yield stiffness, while structures A and B have a high yield strength P_{y2}, and structures C and D have a low yield strength P_{y1}. Structures E and F have a low pre-yield stiffness and a low yield strength P_{y1} (n.b., for simplicity, structures C through F are assumed to have the same yield strength). Structures A and C have the same high ductility, and structure E has the highest ductility, while structures B, D and F have zero ductility.

For load L lower than the yield strength P_{y1}, structures A, B, C and D exhibit the same and small deformation δ, while structures E and F exhibit the same but larger δ. The behaviour of structures E and F is of ordinary soil structures in comparison with steel and RC structures (i.e., structures A, B, C and D).

In dynamic behaviour, when the load L exceeds the resistance P available at a given δ, the difference L - P is resisted by the inertia force of the structure. After yielding, a low value of P results in a large value of L - P with large deformation as obtained by double integration of the acceleration.

As the load L exceeds P_{y1}, δ of structure D becomes larger than that of structure C, and δ of structure F becomes larger than that of structure E. The difference increases with the difference L - P_{y1}. As the load L exceeds P_{y2}, δ of structure B becomes larger than that of structure A. It is specified in the current design codes for RC structures that the shear behaviour of columns and piers should be, comparatively, like that of structure B and the bending behaviour should be like that of structure C so that shear failure does not occur before bending failure occurs; in other words, if failure occurs, it should be bending failure, exhibiting sufficiently ductile behaviour.

At and near JR Rokko-michi Station (see Fig. 4), most of the RC columns of the elevated RC frame structures were seriously damaged or totally collapsed by shear failure. Adjacent to these structures, both sides of the railway embankment were supported by inverted T-shaped RC RWs without a pile foundation. A part of the RWs moved at the base only about 10 cm and/or tilted outward slightly for an angle of about 2 degree (Fig. 7d). When L exceeds P_{y2}, δ of structure B could become larger than that of structure E. If such RC columns which exhibited shear failure can be modeled by structure B, these RC RWs could be modeled by structure E.

The illustrations described above suggest that, for loads exceeding the yield strength, large ductility could be more important than large pre-yield stiffness. It is also understood that it is not enough for a structure to have a reasonably high yield strength and pre-yield stiffness so that it does not exhibit too large displacements against moderate seismic loads. The structure should also be ductile enough as not to totally collapse by very large seismic loads.

On the other hand, failure is brittle for soil structures exhibiting flow failure due to soil liquefaction, for structures resting on liquefying sub-soil deposits and for gravity type RWs exhibiting overturning failure. These structures could be modeled by structure F. This type of structure has the lowest seismic stability for any level of load.

2.3 *Natural slopes*

The earthquake did not seriously damage natural slopes except one landslide at Nikawa, Nishinomiya City, where 11 houses were destroyed and 34 persons were killed. Sassa et al. (1996) summarized locations of the landslides (Fig. 15) and reported that their distribution overlapped that of aftershocks, which were not inversely proportional to the

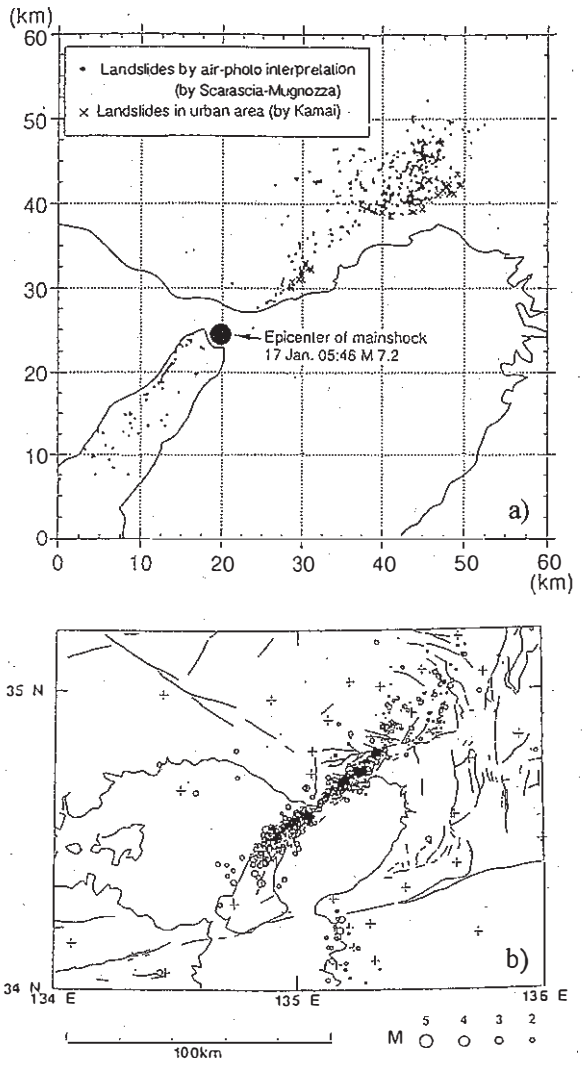

Fig. 15 Distributions of a) slope failures and land slides and b) aftershocks (after Sassa, et al., 1996).

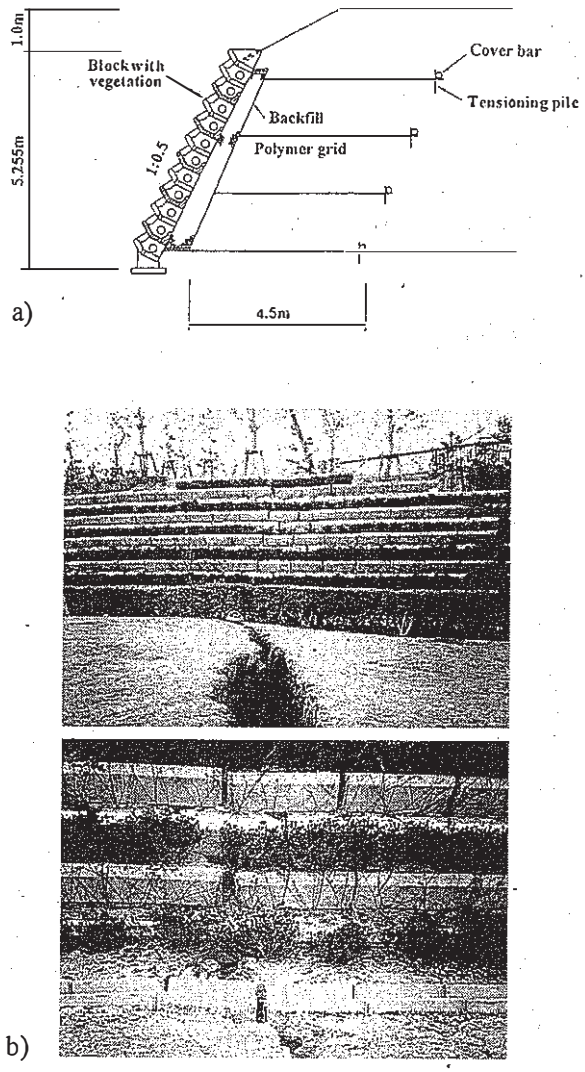

Fig. 16 a) Cross-section and b) front views of the GRS-RW at Maihama Park, Ashiya City (GR2 in Fig. 4) (after Naemura and Miyatake, 1995).

epicentral distance, but rather distributed linearly along active faults. Many of them occurred in the region of Mt. Rokko, which was outside the most severely shaken areas shown in Fig. 4, and the size of each case was not extensive. Based on these observations, it seems that slopes which had been nearly at critical condition at the time of the earthquake suffered from failure by relatively low earthquake motion in the mountain areas. Relatively low ground water level due to the driest season of the year may have contributed to reducing both the number of slope failures and landslides and their extent as pointed out by Sassa et al. (1996).

3 PERFORMANCE OF GEOTEXTILE-REINFORCED SOIL RETAINING WALLS

3.1 *GRS-RWs without full-height rigid facings*

Around the periphery of the most severely shaken areas (see Fig. 4), several types of geotextile-reinforced soil retaining walls (GRS-RWs) without full-height rigid (FHR) facings was constructed as secondary applications.

Fig. 16 (GR2 in Fig. 4) shows a GRS-RW that was constructed in May 1993 at Maihama Park in a reclaimed land (Naemura and Miyatake, 1995). The wall was 5.0 m high and 90 m long. The facing was inclined at 0.5:1.0 in horizontal:vertical. The

reinforcement was a high density polymer grid (the tradename is Tensar SR-55) having a nominal tensile strength of 49 kN/m (5 tonf/m). The reinforcement was on average 4.5 m in length with a vertical spacing of 1.4 m. The facing was a stack of discrete concrete blocks having a hollow core with vegetation inside. The facing was not connected with the reinforced backfill, but separated by a layer of gravel.

Noticeable soil liquefaction occurred in the subsoil in front of the wall. The ground settled unevenly with cracks, from which sand and water erupted. One large crack reached to the subsoil below the facing blocks, which resulted in a separation between adjacent blocks of about 10 cm and noticeable unequal settlement of the facing. Yet, the deformation of the facing was smaller than that in the subsoil, and the integrity of the facing and backfill was maintained. In fact, the wall has been in service since the earthquake.

Fig. 17 (GR3 in Fig. 3) shows another GRS-RW, similar to the above, which was constructed in September 1993, along the west-side slope of an approach road to Akashi Kaikyo Bridge (MKS, 1995, Nishimura et al., 1996). The wall was 4 m high and 95 m long. The reinforcement was Tensar SR-55, as for the aforementioned GRS-RW, and the facing consisted of L-shaped steel wire frame. On the ground surface in front of the wall, cracks with a maximum opening of 20 cm appeared, and an unequal settlement of about 20 cm was observed. One of the construction joints of the foundation for noise barrier walls on top of the GRS-RW exhibited a lateral shear displacement of about 2 cm. Despite the above, no problematic deformation of the GRS-RW was noticed.

These two case histories show some ductility of GRS-RWs in comparison with the catastrophic brittle failure of several unreinforced embankments triggered by the soil liquefaction in the subsoil (as listed in Table 2).

3.2. *GRS-RWs having full-height rigid facings*

GRS-RWs having full-height rigid (FHR) facings were constructed at four locations in 1990 - 1994 in the affected area (marked by symbols ◎ in Fig. 3). The walls had been aseismic-designed using $k_h = 0.2$. These GRS-RWs were constructed by following the staged construction procedures shown in Fig. 18 (Tatsuoka et al., 1992, 1996c). The reinforcement was a grid made of fibers of polyvinyl alcohol (the tradename is Vinylon) coated with soft PVC for protection, with a nearly rectangular cross-section of 2 mm times 1 mm and an aperture of 20 mm. The

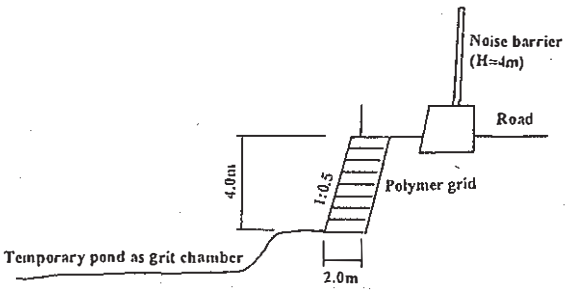

Fig. 17 Cross-section of the GRS-RW along the west-side slope of one of the approach roads to Akashi Kaikyo Bridge (GR3 in Fig. 3; after Mitsubishi Yuka Sanshi Products Co.,Ltd., 1995).

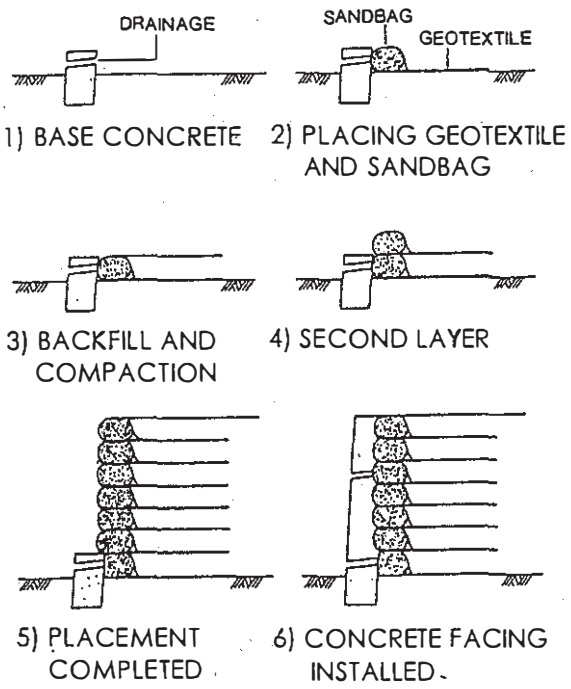

Fig. 18 Standard staged construction procedures for GRS-RWs having full-height rigid facings.

nominal tensile rupture strength is 29 kN/m (3tonf/m). The following three walls were located in the areas where the JMA scale was fifth or sixth:

a) Amagasaki, No. 1 (Fig. 19; wall height H= 5 m on average and total length L= about 1 km): The wall was completed in April 1992 to support two new tracks added on both sides of an existing railway embankment of the JR Kobe Line (GR4 in Fig. 3). The backfill was as basically a cohesionless soil including a small amount of fines. A number of foundations for a steel frame structure for electricity supply had been constructed inside the reinforced backfill. Four pairs of bridge abutments of GRS-RW had been constructed. No deformation of the wall by the earthquake was observed.

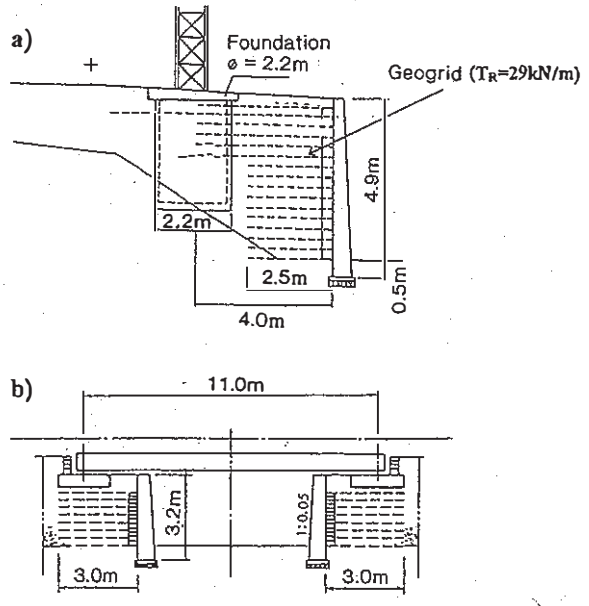

Fig. 19 a) Typical cross-section of Amagasaki No. 1 GRS-RW and b) typical GRS bridge abutments (GR4 in Fig. 3).

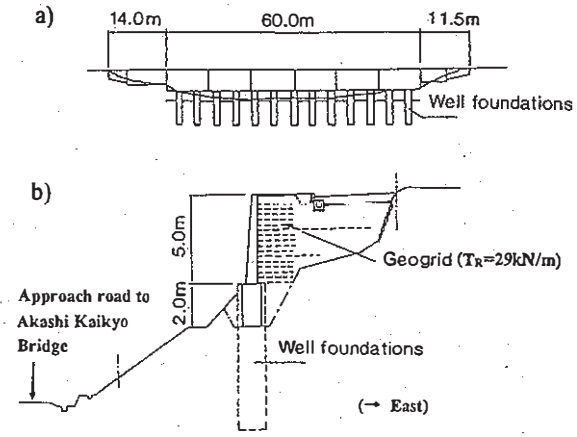

Fig. 20 a) Front view and b) cross-section of Tarumi GRS-RW (Block B) (GR5 in Fig. 3).

b) Maiko at Tarumi-ku, Kobe City (GR5 in Fig. 3): The wall having Blocks A and B, constructed in 1993 to expand the road immediately east of one of the approach roads to Akashi Kaikyo (Strait) Bridge. The backfill was a well-graded gravel. On the opposite side of the approach road, there exists the GRS-RW without a FHR facing described in section 3.1. Block B (Fig. 20; H= 4.9 - 5.1 m and L= 60 m) was located on a steep slope facing the approach road. The facing was supported with well foundations. The wall moved outward about 2 cm at a maximum at the top of the facing. Block A (Fig. 21; H= 3.7 - 6.6 m and L= 55 m), facing the direction opposite to the approach road, moved outward about 1 cm relative to the low-height gravity type RW immediately to the right of the GRS-RW in Fig.21a. On the left of the GRS-RW in Fig. 21a, a RC wall had been constructed, supported by steel pipe piles (Fig. 21c). Although the height of the RC wall was shorter than that of the GRS-RW, it moved outward about 2 cm relative to the GRS-RW showing a maximum depression of about 10 cm at the road face behind the RC wall. This fact indicates that RC RWs supported by piles could be less cost-effective in terms of seismic stability than GRS-RWs having FHR facings. A similar case was observed on a larger scale at Tanata, to be described later. The displacement of the masonry walls on the left end and the gravity type RW on the right end was not observed, probably due to their small height (about 2.2 m). No further displacement was observed after the earthquake in all these walls.

c) Amagasaki, No. 2 (Fig. 22) (H= 2.0 - 8.0 m and L= 500 m; GR6 in Fig. 3): The site is west of the Amagasaki No. 1 GRS-RW, adjacent to Amagasaki Station (Fig. 19). The wall was completed in March 1994 for the JR Fukuchiyama Line. No displacement of the wall by the earthquake was observed.

In the areas adjacent to these GRS-RWs having FHR facings, a number of wooden houses, railway and highway embankments and conventional types of RWs were seriously damaged (see Fig. 3). The degree of damage was, however, not as serious as that observed in the areas where the JMA scale was equal to seventh or higher (Fig. 4). In one of these areas, at Mori-Minami-cho 1-chome in Higashi-Nada-ku, Kobe City (the local name is Tanata), GRS-RWs having FHR facings (H= 1.5 m - 6 m and L= 305 m) were completed in February 1992 on the south slope of the embankment of JR Kobe Line (Fig. 23; GR1 in Fig. 4). The wall construction was to increase the number of railway tracks from four to five (Figs. 23a and b). The subsoil condition is relatively good (see Figs. 23d and e). In sections where the wall was higher than 1.5 m, H-shaped steel piles at a spacing of 1.5 m with temporary anchors were provided at two elevations to retain the embankment before the slope was excavated for the construction of the wall (Fig. 23d). The anchors were removed as the GRS-RWs were being constructed.

The bottom of the wall moved outward on average about 5 cm relative to the supporting foundation subsoil, pushing the subsoil in front of the wall laterally. At the highest part of the wall, which was in contact with a RC box culvert structure crossing the railway embankment, the largest outward displacement occurred, which was 26 cm at the top of the wall and 10 cm at the ground surface level (Fig. 24a).

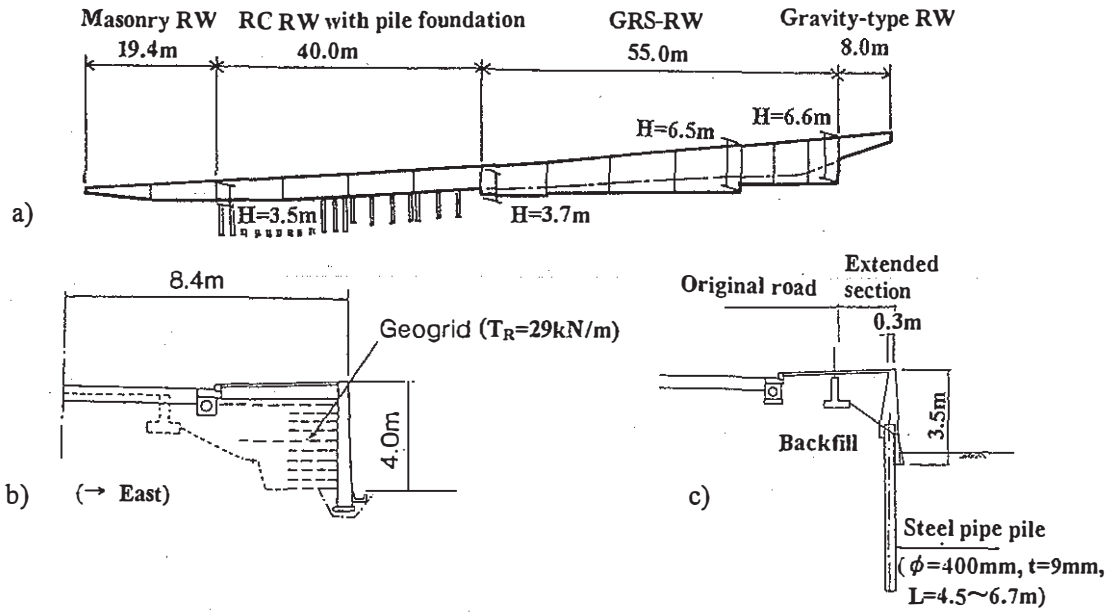

Fig. 21 a) Front view and b) cross-section of Tarumi GRS-RW (Block A) (GR5 in Fig. 3) and c) cross-section of the adjacent RC RW with piles.

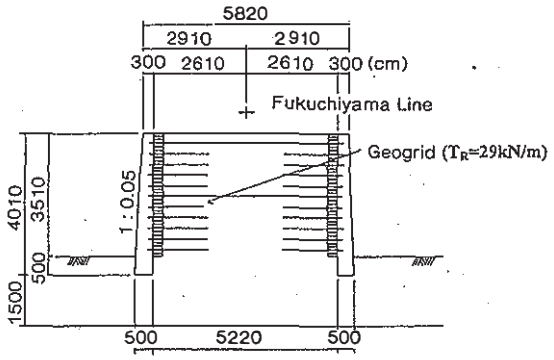

Fig. 22 Typical cross-section of Amagasaki No. 2 GRS-RW (GR6 in Fig. 3).

Despite the noticeable movement of the wall, the performance of the GRS-RW walls were considered quite satisfactory for the following reasons;

a) At the site and in the adjacent areas, the seismic intensity was extra-ordinarily high (Fig. 4). More than 80 % of the wooden houses in front of the wall totally collapsed, but most of them were not particularly old (Fig. 25). In the areas surrounding the wall, many RC buildings and RC piers for highways were seriously damaged or totally collapsed. No doubt, this GRS-RW experienced the highest seismic load among the modern GRS-RWs.

b) On the opposite side of the RC box structure, a RC RW with a largest height of about 6 m was constructed concurrently with the GRS-RW (Fig. 23e). The wall was supported by a row of bored piles, despite the sub-surface condition was similar to that of the GRS-RW. Consequently, the construction cost per wall length for the RC RW was about double to triple that for the GRS-RW. The RC RW displaced similarly to the GRS-RW; i.e., at the interface with the side of the RC box structure, the outward lateral displacement was 21.5 cm at the top and 10 cm at the ground surface level (Fig. 24b). This comparable behaviour of these two different types of RWs constructed adjacent to each other was similar to that at Maiko described above. Moreover, the GRS-RW having a FHR facing had been constructed adjacent to and to the west of the RC RW (see Fig. 23a), which was 3 m high and 45 m long. The wall did not move. In the design of RC RWs, such as the one at Tanata, seismic earth pressure calculated by the Mononobe-Okabe method using k_h= 0.2 is resisted by the lateral and rotational resistance of the pile foundation, which results mainly from passive earth pressure in the subsoil in front of the pile foundation. Therefore, some lateral displacement of the pile was inevitable to mobilize the large passive earth pressure.

c) The design standard for railway earth structures (Ministry of Transport, 1992) specifies the minimum allowable length of grid reinforcement for the GRS-RW system to be the larger value of either 35 % of the wall height or 1.5 m. For most of the GRS-RWs constructed so far, to be conservative, several top reinforcement layers were made longer than the others at lower levels (Figs. 19, 20 and 21). For the Tanata GRS-RW, however, all the reinforcement layers were truncated to nearly the same length (Fig. 23d). That was due to a construction constraint to allow trains to run in the area where the top several reinforcement layers should have been extended. This arrangement may have reduced the seismic

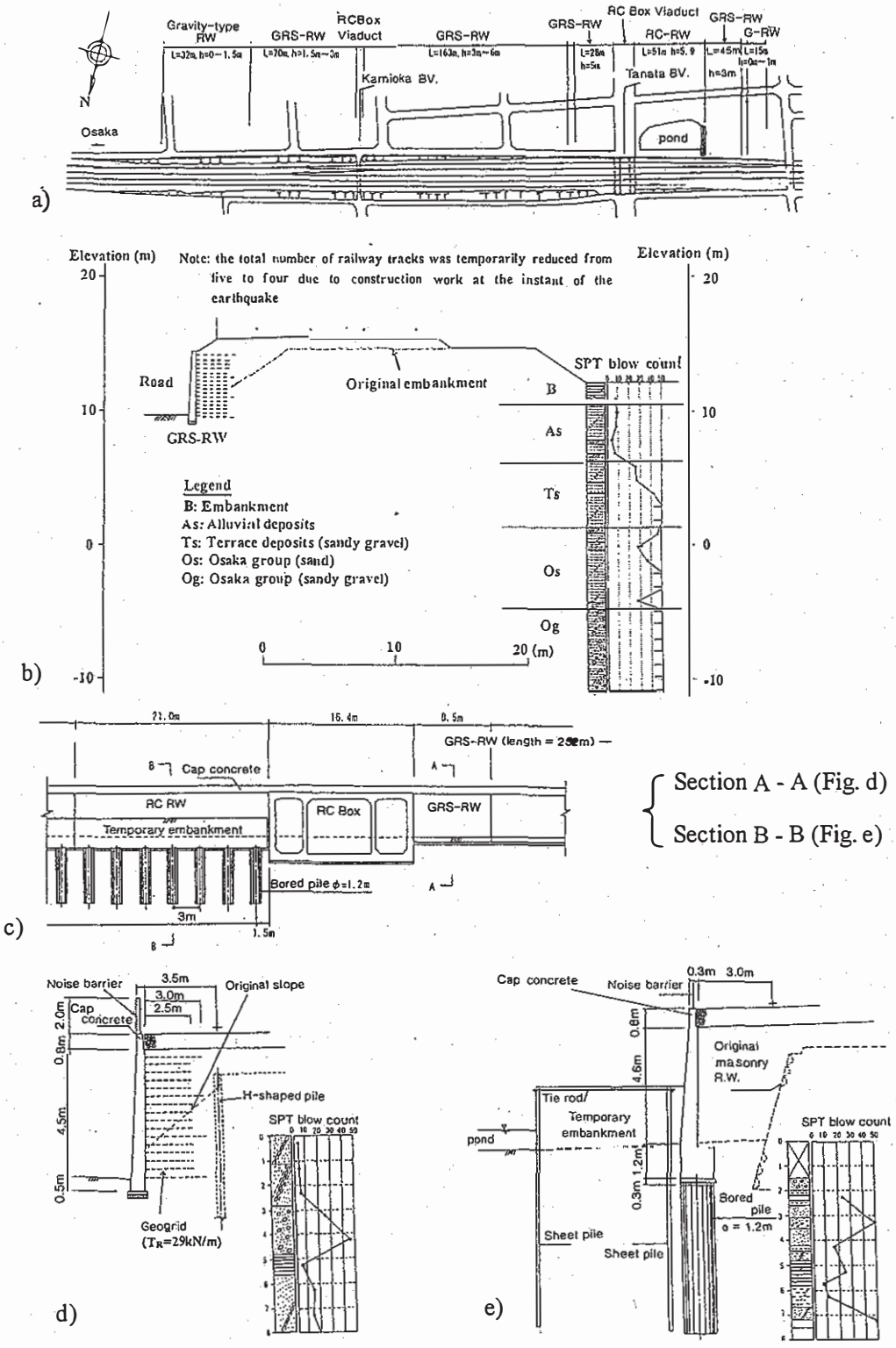

Fig. 23 a) Plan, b) cross-section of the embankment and c) front view from the south and cross-sections of d) GRS-RW and e) RC RW with pile (GR1 in Fig. 4), at Tanata between Ashiya and Setsu-motoyama Stations, JR Kobe Line.

stability of the wall, particularly in terms of overturning.

It is very likely that GRS-RWs having FHR facings would not have collapsed even if they had been constructed on liquefying sub-soil. Murata et al. (1994) performed a shaking table test under plane strain conditions of a large model GRS-RW con-

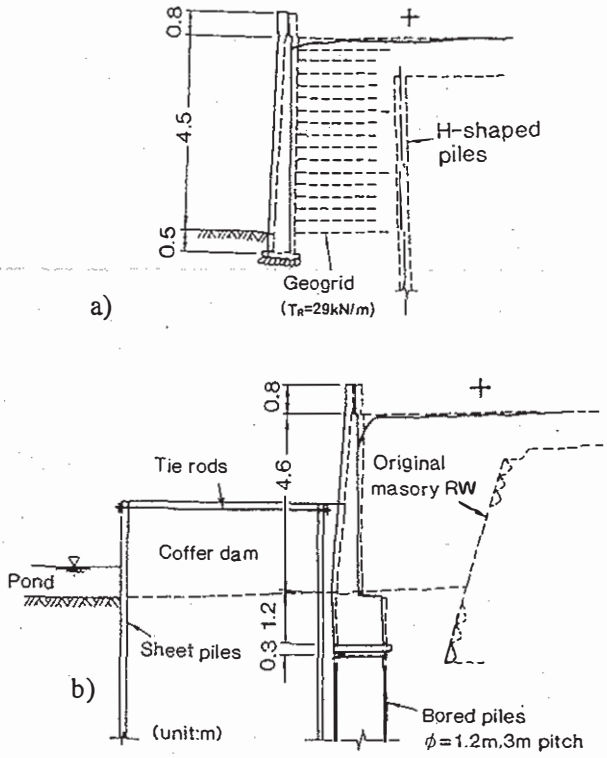

Fig. 24 Deformation due to the earthquake of a) GRS-RW and b) RC RW with piles at Tanata.

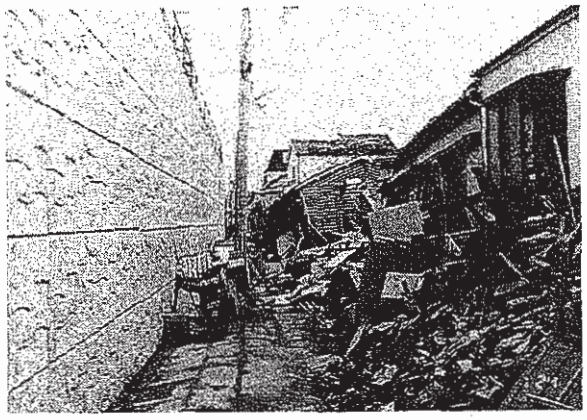

Fig. 25 View in front of the GRS-RW immediately after the earthquake

structed on a saturated sand layer (Fig. 26). The sand zones on both the sides of the wall liquefied by the application of 360 cycles of sinusoidal loads at a frequency of 2 Hz with a peak acceleration of 400 cm/sec^2. It seems that the sand zone beneath the center of the wall did not liquefy due to the weight of the wall, as seen from the excess pore water pressure recorded beneath the center of the wall. As a result, the facings settled about 2cm relative to the reinforced backfill, but the wall maintained its integrity. This result suggests that when the foundation subsoil liquefies, a GRS-RW having a FHR facing will deform and displace more than when the subsoil does not liquefy, but may not totally collapse.

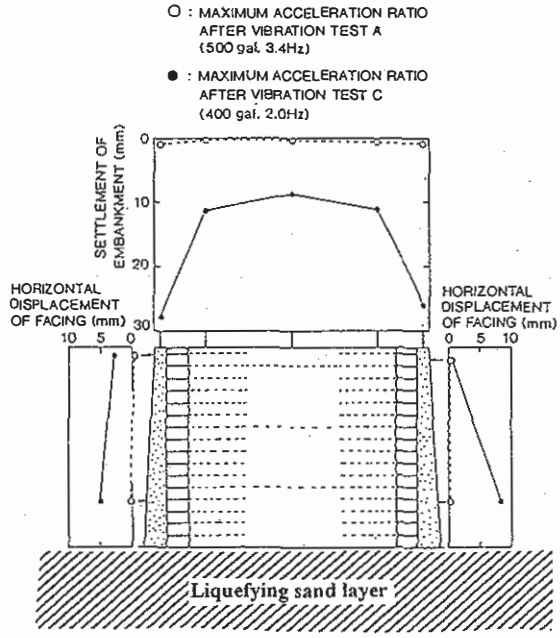

Fig. 26 Deformation of a large GRS-RW model constructed on a liquefied sand deposit (after Fig. 5 of Murata et al., 1994).

4 PERFORMANCE OF STEEL-REINFORCED SOIL RETAINING WALLS

4.1 *Terre Armee walls*

Among other types of permanent reinforced soil RWs that had been constructed in the areas affected by the earthquake, Terre Armee walls had the largest number; 66 walls had been constructed within a radius of 70 km from the epicenter. Although they were located outside the most severely shaken areas where the JMA scale was equal to seventh or higher, several walls had been constructed in the next most severely shaken areas with a JMA scale equal to sixth. They exhibited high seismic resistance without any total collapse. However, three walls exhibited relatively large deformation as the GRS-RW at Tanata, and one of them was partly reconstructed after the earthquake.

Fig. 27 shows a relatively large scale Terre Armee RW that was completed in January 1994 in Awaji Island (TA1 in Fig. 3) as a part of the approach road

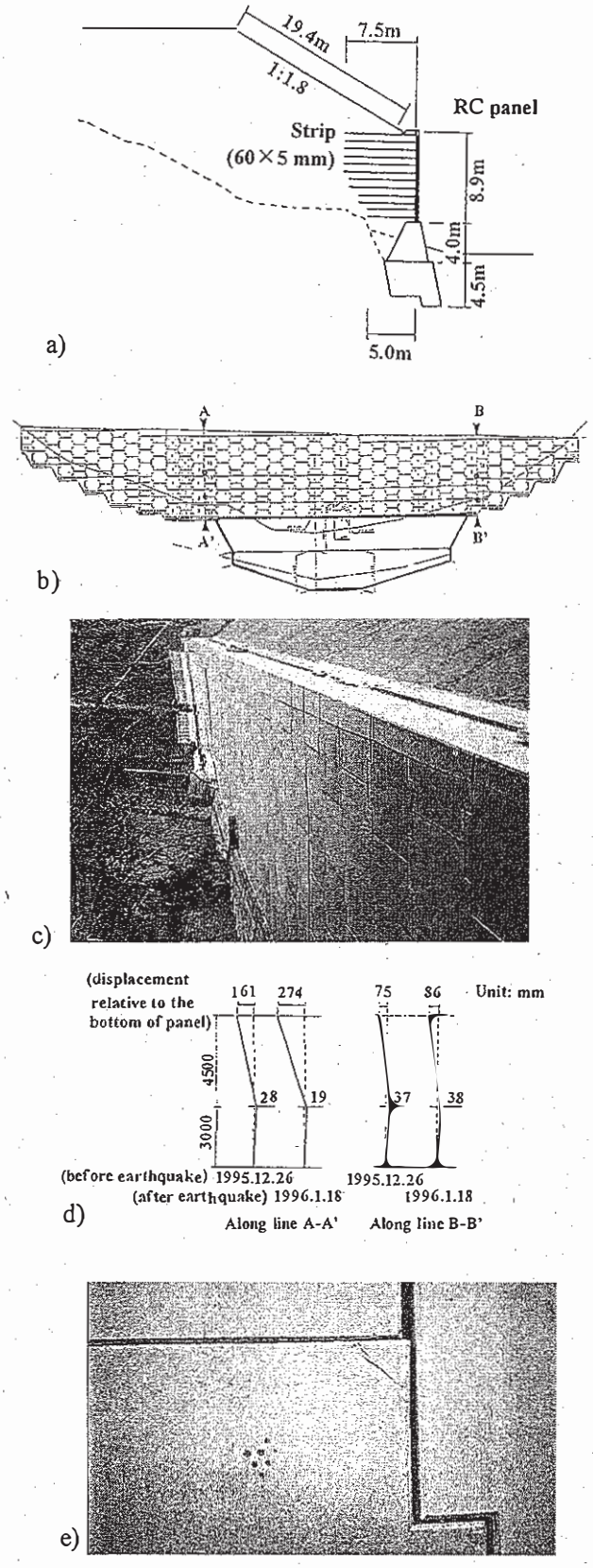

Fig. 27 a) Cross-section, b) front view, c) general view, d) wall deformation and e) cracking at the corners of RC panel, Terre Armee wall in Awaji Island (TA1 in Fig. 3) (JTAA, 1995).

(National road No. 28) to Akashi Kaikyo bridge (JTAA, 1995). The largest wall height was 9 m and the total wall area was 464 m^2. The backfill soil is a medium-grained sand including fines less than 20%. The facing consisted of discrete precast RC panels. The wall had been aseismic-designed by the pseudo-static stability analysis using k_h= 0.15. The largest overhanging of 27.4 cm at the top of the facing relative to a level of 4.5 m down from the top was found after the earthquake (Fig. 27d). About a half of that deformation was considered due to the earthquake. Corner portions of some panels cracked (Fig. 27e), probably due to relative movements between the adjacent panels during the earthquake.

According to the information obtained by the authors, for conservatism, the top 4.5 m height for the entire wall length was reconstructed by increasing the length of the top six reinforcement layers from 7 m to 9 m aiming at increasing the pull-out resistance. This re-arrangement was based on another pseudo-static stability analysis using k_h= 0.4.

Fig. 28 (TA2 in Fig. 3) shows another Terre Armee RW, which has two continuous wall faces bending at a right angle at the center (JTAA, 1995). The RW was retaining an earthfill for Hoshiga-oka Park of Kobe City, completed in November 1989. The largest wall height and total wall area were, respectively, 4.5 m and 162.7 m^2. The backfill was a gravelly soil. The wall exhibited relatively large deformation and displacement. Note that a masonry wall located 100 m from the site collapsed totally (Fig.29). The largest overall outward movement of the facing relative to the facing bottom was reported to be about 9 cm. However, from the fact that the largest lateral opening between adjacent panels was about 20 cm (Fig. 28e) and a number of openings with noticeable widths appeared on the crest on the backfill (Fig. 28f), it is very likely that the whole wall moved outward much more than 9 cm. Also for this wall, corner portions of some RC panels cracked.

Fig. 30 (TA3 in Fig. 3) shows another permanent Terre Armee RW which exhibited relatively large deformation (JTAA, 1995, Matsui et al., 1996). This wall was completed in June 1980, having a largest wall height of 3.27 m and a total wall area of 120 m^2. The top of the wall moved outward 94 mm at the largest. However, considering the fact that the top surface of the backfill settled 20 cm to 100 cm, it is very likely that the base of the facing also moved outward to some extent. Also for this wall, corner portions of some RC panels cracked (Fig. 30g).

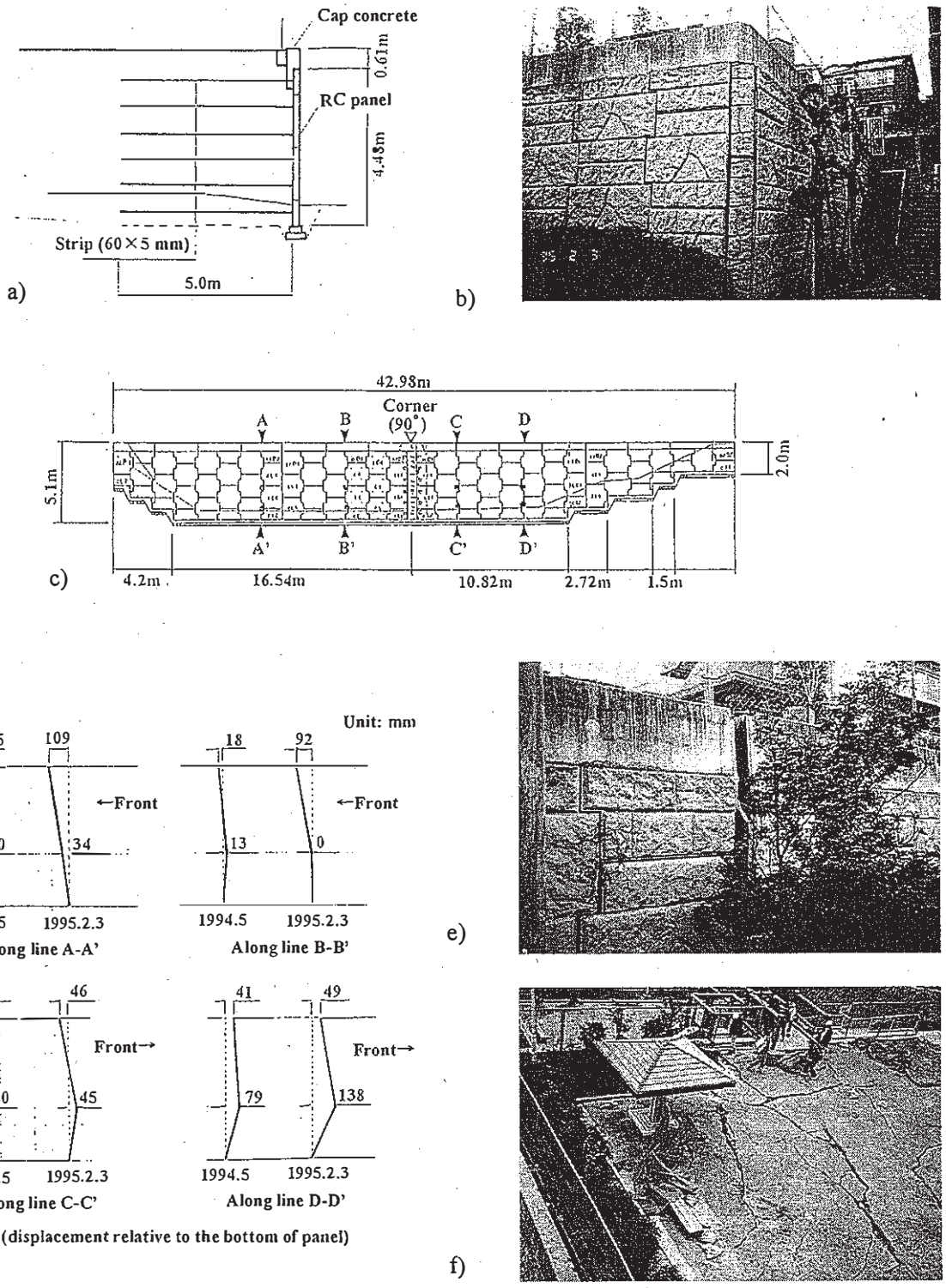

Fig. 28 a) Cross-section, b) general view, c) expanded front view, d) wall deformation, e) opening at a vertical construction joint and f) cracking on the embankment surface, Terre Armee wall for Hosiga-oka Park, Kobe City (TA2 in Fig. 3) (JTAA, 1995).

Fig. 29 A collapsed masonry wall located near the Terre Armee wall TA2 (JTAA, 1995)

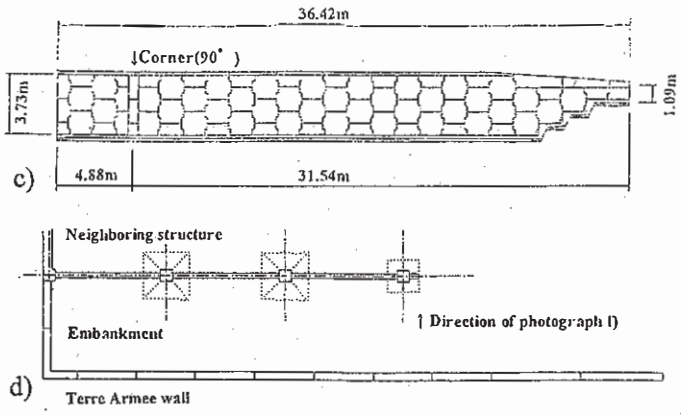

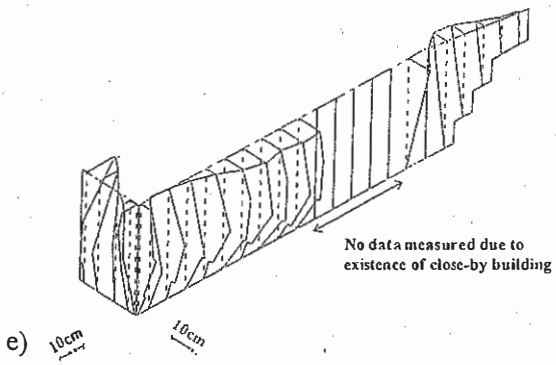

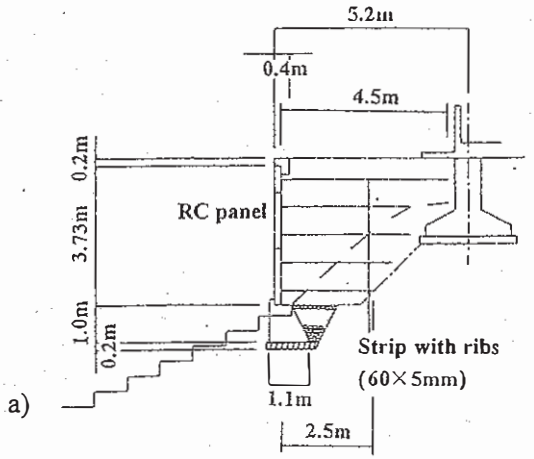

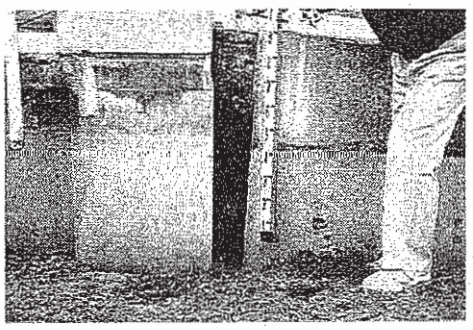

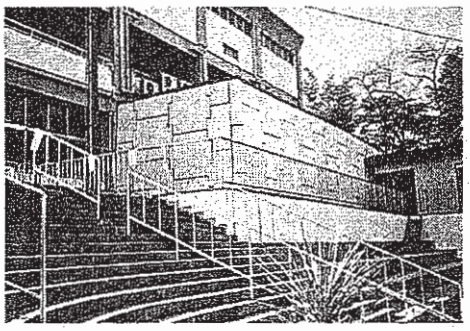

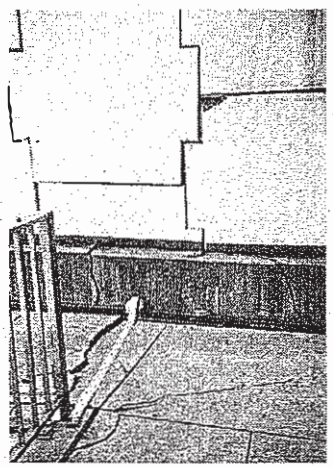

Fig. 30 a) Cross-section, b) general view, c) expanded front view, d) plan, e) wall deformation, f) settlement of embankment relative to the neighboring structure, and g) cracking of the corner of RC panel, Terre Armee wall at Itami City (TA3 in Fig. 3) (JTAA, 1995, Matsui et al., 1996).

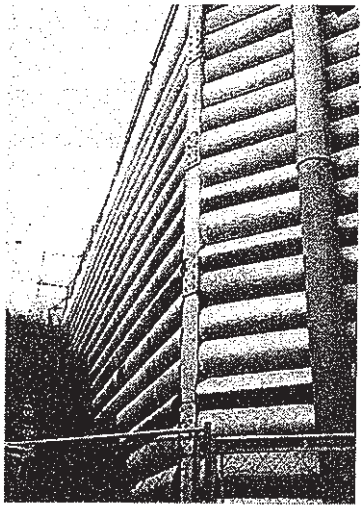

Fig. 31 Temporary Terre Armee wall at Tarumi-ku (by the courtesy of Prof. Akagi, T. of Toyo University).

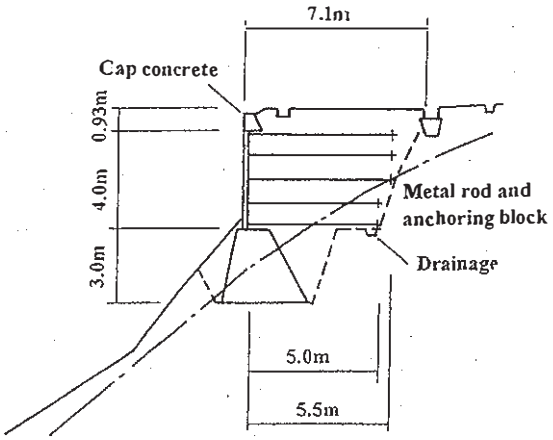

Fig. 32 Cross-section of a multiple-anchor soil RW (MA in Fig. 3).

There was a 6 -7 m high temporary Terre Armee wall with a metal skin facing at Tarumi-ku for the construction of an approach road to Akashi Kaikyo Bridge. Some part of the facing, particularly near the bottom, was compressed noticeably (Fig. 31, TA4 in Fig. 3), inducing some outward displacement and settlement at the entire wall. As the wall did not show any sign of total collapse, only some remedy work was performed.

In summary, the Terre Armee RWs generally behaved very well. The RWs are made relatively deformable by using a discrete panel facing to accommodate possible deformation of the subsoil and backfill. It seems that because of the above, the walls deformed to some extent during the earthquake to a higher level than the conventional RC walls that were stable during the earthquake and the GRS-RWs having FHR facings. Cracks observed at the corner potions of RC panels suggest the above. The ductile behaviour of the wall may have contributed to avoiding total collapse by reducing the seismic response presumably due to large energy absorption by the backfill and the dynamic earth pressure exerting on the back face of the reinforced zone. It seems that as a result, the residual deformation has become larger.

4.2 *Other types of walls*

In the mountain areas, where the seismic intensity was lower than in the areas shown in Fig. 4, some multiple-anchor soil RWs had been constructed. Precast RC panels were anchored with steel tie rods having small anchor concrete blocks at the deepest ends. The wall shown in Fig. 32 (MA in Fig. 3) had a largest wall height of 4.6 m and a total wall area of 87 m^2 (JMAA, 1995). No structural damage and deformation was observed at the wall face, but the cap concrete, that was not anchored, moved backward slightly.

5 PERFORMANCE OF REINFORCED NATURAL SLOPES

5.1 *Nailed slopes*

Felio et al. (1990) reported good performance of eight nailed slopes during the 1989 Loma Prieta earthquake. Torii (1996) summarized the performance of seven nailed slopes during this earthquake (Table 3 and Fig. 33a). The PHGAs listed in Table 3 were estimated from the PHGA contours shown in Fig. 33b. It is reported that no noticeable deformation of the nailed slopes was observed despite relatively high PHGAs, which was in contrast to serious damage to adjacent civil engineering structures and unreinforced slopes (except the one case described below).

Among them, perhaps the behaviour of the nailed wall NS6 (Fig.3) was most carefully monitored at the time of the earthquake. The slope was in the process of excavation while having exhibited noticeable deformation (Fig. 34) (Fujii et al., 1996). The wall was nearly vertical while the soil was not very stiff. At the time of the earthquake, the slope had been excavated to a depth about 4.0 - 5.0 m. The wall displaced outward 1.9 mm and 3.2 mm at the largest at the measuring sections Nos. 1 and 2, showing an overturning mode as observed before and after the earthquake. No damage to the houses and other structures in the adjacent areas was observed,

Table 3 List of the nailed slopes located in the affected areas (see Fig. 33) (after Torii,T., Research Committee on Reinforcement Technology for Natural Slopes, 1996).

No.	Slope height and wall area	Slope (V:H)	Soil type	Reinforcement Material	(mm)	(m)	(m)	Facing	Permanent Spacing temporary	Esti-mated PHGA
NS1	20 (m) ---* (m^2)	1:0.5	Weathered granite	Threaded deformed steel bar (TD bar)	25	V: 1.25 H: -	5.0	Shotcrete thichness t= 50 (mm)	Permanent	350 (gals)
NS2	4	1:0.4	Decomposed granaite	TD bar	29	V: 1.5 H: -	4.0	Precast RC panels t= 300	Permanent	300
NS3	3	1:0.4	Holocene sand	TD bar	-	V: 1.5 H: -	5.5	Precast RC panels t= 300	Permanent	700
NS4	10	1:0.3	Terrace gravel/ weathered granite	Deformed steel bar (D bar)	22	V: 1.5 H: 1.5	6.8	Shotcrete t= 100	Temporary	500
NS5	7	1:0.6	Terrace gravel/ weathered granite	D bar	22	V: 1.5 H: 1.5	4.0	Shotcrete t= 100	Permanent	500
NS6	5m at the time of earthquake (final 14.3m)	1:0.1	Pleisto-cene sand and clay	D bar	22	V: 1.5 H: 1.5	5.5-6.2	Shotcrete t= 100	Temporary	200
NS7	Total 16m (backfilled by concrete to a height of 6.4m)	1:0.2	Granite covered with debris	D bar	25	V: 1.5 H: 1.4	3-7	Shotcrete t= 150 with lattice RC frame as leaning type RW	Permanent	600 (PVGA =300)

*) not reported

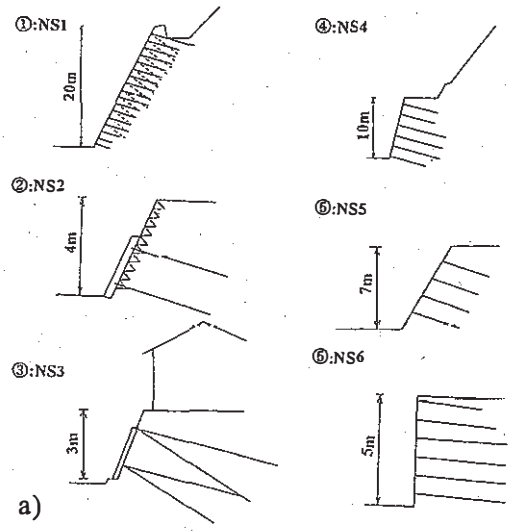

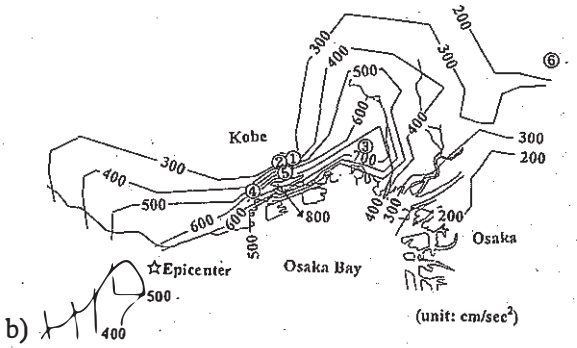

Fig. 33 a) Cross-sections of the nailed slopes listed in Table 3 and b) locations of the nailed slopes and contours of estimated PHGA (according to Ohbayashi Corp., 1995) (after Torii,T., Research Committee on Reinforcement Technology for Natural Slopes, 1996).

because the site was a bit far away from the epicenter and the estimated PHGA was relatively low. It seems that the slope was already near the critical state at the time of the earthquake, and the slope would have not been stable without nailing during the earthquake. Despite higher PHGAs, the other slopes were more stable probably due to better soil conditions and/or larger inclination of the slopes.

A nailed slope located in Awaji Island (NS7 in Fig.3), on an approach road to Akashi Kaikyo Bridge, was located closest to the epicenter (Fig. 35). Before the earthquake, some deformation of the excavated slope face had been noticed after having excavated to the bottom of the slope. Therefore, two layers of ground anchor had been installed at depths of 8.7 m and 11.6 m from the slope crest. After well foundations were constructed in front of the slope, the space between the slope face and the back face of the well foundation had been backfilled with

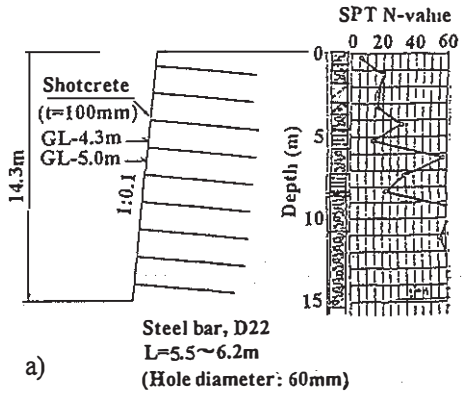

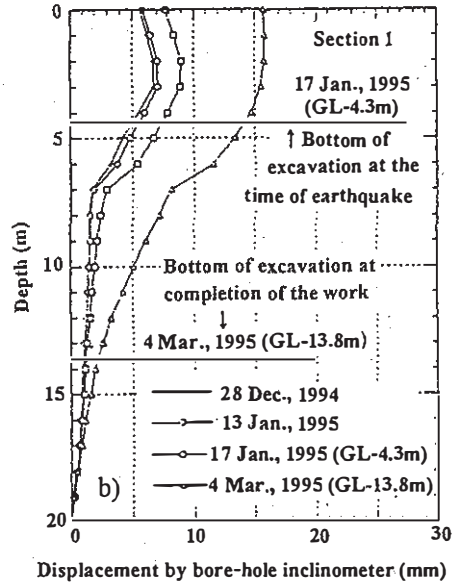

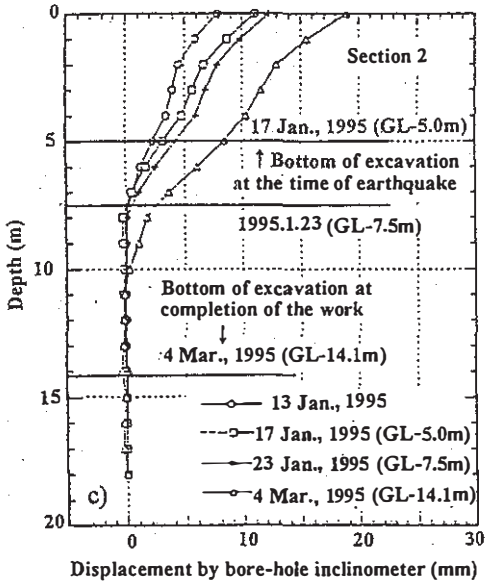

Fig. 34 a) Cross-section at the end of excavation and b) displacements at the slope face of the nailed slope NS6 in Fig. 3 (Fujii et al., 1996).

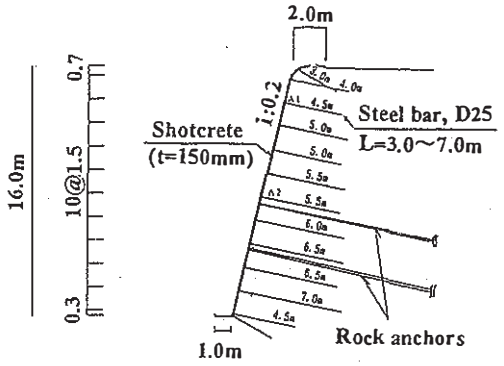

Fig. 35 Cross-section of a nailed slope in Awaji Island (NS7 in Fig. 3; Tsukuda et al., 1996).

concrete up to a depth of 9.6 m from the slope crest by the time of the earthquake. The results of pseudo-static seismic analysis performed after the earthquake for the slope with and without nailing showed that the slope had become more stable by nailing (Tsukuda et al., 1996). Although the reinforced slope was not damaged by the earthquake, a safety factor equal to 0.8 was obtained when applying k_h= 0.6, which is equal to the estimated PHGA/g, normal to the slope face. They considered that this discrepancy was due to the fact that the direction of the PHGA was largely inclined (more than 60 degrees) from the normal to the slope surface. The authors consider, however, that many other factors should be considered as well.

Root-piled slopes: Ten slopes had been stabilized by the root pile technique in the areas where the estimated PHGA was 100 gals or more (Fujii et al., 1996). Among them, the following two cases are important.

A slope located north-east of Suma-koen Station of the Sanyo Dentetsu railway (RP1; Fig. 36) (see Fig. 3) experienced an estimated PHGA of about 500 gals. A 6 - 7 m high slope had been stabilized by root piling, adjacent to a 1 - 3 m high slope that had been retained only by a masonry RW. The slope was of a residual soil, basically a gravelly sand with inter-bedded clay. The root-piled slope had two different facings, masonry and shotcrete. A number of hair cracks were observed on the shotcrete facing and on the road face behind the wall face, and an opening of 5 cm appeared between the masonry and shotcrete facings. However, the damage was not serious at all. The deformation of the masonry facing was smaller. Compared with the above, the masonry facing of the unstabilized slope collapsed, and several nearby wooden houses were seriously damaged.

In the second case located south of JR Takarazuka Station on the right bank of Mukogawa river (RP2 in Fig. 3; Fig. 37), the estimated PHGA was about 500

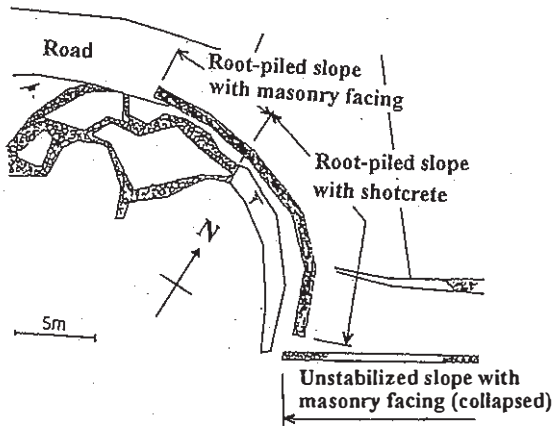

Fig. 36 Plan of the root-piled slopes and adjacent damaged unreinforced slope near Suma-Koen (RP1 in Fig. 3; after Fujii et al., 1996).

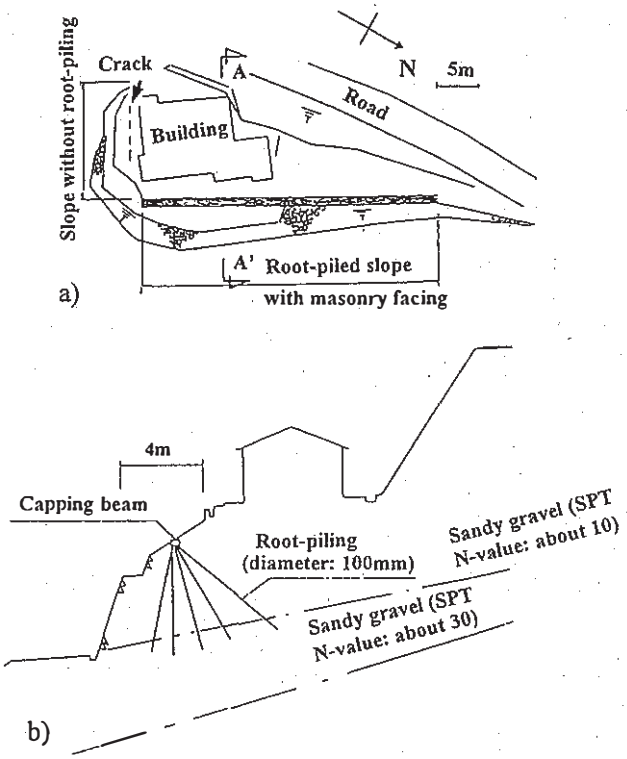

Fig. 37 a) Plan of the root-piled slope and adjacent damaged unreinforced slopes and b) cross-section A-A' of the root-piled slope near Takarazuka (RP2 in Fig. 3; after Fujii et al., 1996).

gals. An about 7 m high slope having a masonry RW had been stabilized by root piling, while the adjacent slope with a height of 5.0 m at the maximum had been retained only by a masonry RW. The slope soil was basically a sandy gravel. In the root-piled slope, the soil mass between the wall face and the root piles seems to have moved slightly outward while the root-piled zone and the soil behind it did not, judging from some small cracks and no cracks on the ground surfaces, respectively, in front of and behind the capping beam. Compared with the good performance of the root-piled slope, on the crest of the slope without root-piling, a crack with a maximum width of about 20 cm appeared immediately behind the masonry RW, associated with a 7 cm deep depression at a distance of 20 cm from the masonry RW. This fact shows that the unstabilized slope moved outward to a some extent.

These two case histories show relatively high seismic stability of the root-piled slopes compared with the unstabilized slopes. It seems, however, that the stability of the zone in front of root piles would be prone to larger outward displacement when subjected to higher seismic loads. This zone can be stabilized by nailing from the wall face.

6 LESSONS FROM THE CASE HISTORIES AND SOME CONSIDERATIONS ON SEISMIC DESIGN

6.1 *Summary of the seismic behaviour of reinforced RWs*

Fig. 38 is the authors' evaluation of the relative construction cost and seismic performance of several different types of RWs and sloped embankments. From the case histories described in this report, the following conclusions are reached:

1) Among the structures located in the severely shaken areas, all the geosynthetic- and steel-reinforced soil RWs performed better than not only most of the masonry RWs and the gravity and leaning type unreinforced concrete RWs, but also a number of cantilever or inverted T-shaped RC RWs which exhibited large displacements (most of them were not supported by piles). The performance of the reinforced soil RWs was even better than a number of RC columns and piers which collapsed by shear failure. When following the aseismic characterization of structure illustrated in Fig. 14, the masonry RWs and the gravity and leaning type unreinforced concrete RWs are classified as "structure F", the cantilever or inverted T-shaped RC RWs are classified as between "structures E and F", and the RC columns are classified as "structure B".

2) The good seismic performance of the reinforced soil RWs is comparable to that of the cantilever or inverted T-shaped RC RWs which were supported by piles and performed very well. Therefore, both of them could be classified as "structure E". Between the two, the reinforced soil RWs are more cost-effective.

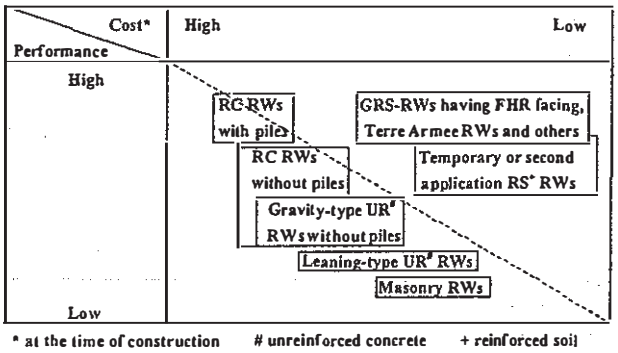

Fig. 38 Approximated evaluation of cost and seismic performance of different types of soil retaining structures.

6.2 *Analysis by current seismic design methods*

The seismic stability of the damaged conventional soil RWs (LT1, GT1, CL2 and CL4 in Fig. 4) and the GRS-RW having a FHR facing at Tanata (GR1 in Fig. 4) was analyzed by limit equilibrium-based pseudo-static stability analysis in the framework of the current seismic design procedure (Koseki et al., 1996). In the analysis, the effects of vertical seismic force was found to be much smaller than those of horizontal seismic force, and therefore will not be discussed herein.

The seismic stability of the GRS-RW was evaluated by the two-wedge method (Fig. 39; Horii et al., 1994). In this method, the same horizontal seismic coefficient is applied to the facing and the reinforced and unreinforced zones of backfill, while no seismic load is applied to the subsoil. The seismic loads are resisted mainly by the tensile force in the reinforcement and partly by the reaction force at the bottom of the facing. Sliding at the base of the facing and reinforced backfill and the overturning of the facing together with the active zone F are also examined. To prevent sliding at the base, several bottom reinforcement layers are made long enough as in the case of RC RWs without a pile foundation. When the safety factor for bearing capacity at the facing base is becoming less than unity, the direction of the earth pressure acting on the back face of the facing is inclined more horizontally so that the safety factor does not become less than unity. The increased tensile force resulting from this procedure is accommodated by rearranging the reinforcement. This methodology was supported by the results of a large-scale shaking test on a GRS-RW model constructed on a liquefiable sand deposit (Fig. 26). In the test, the wall was able to maintain its stability even when the load acting at the bottom of the facing had reached the bearing capacity of the subsoil, which was decreased substantially by liquefaction.

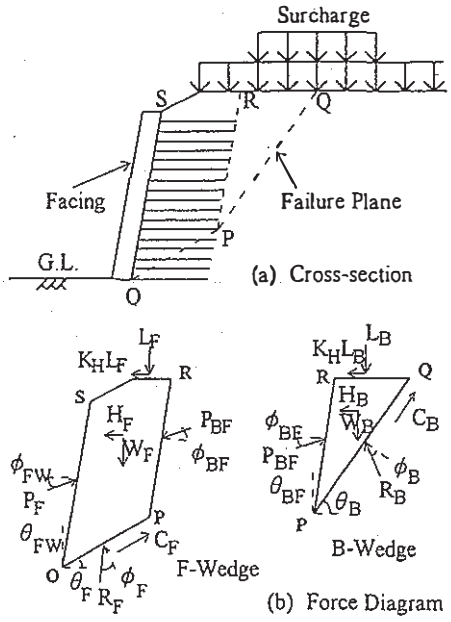

Fig. 39 Two-wedge method to evaluate the seismic stability of GRS-RWs (after Horii et al., 1994).

The design parameters employed in the analysis against external instability are shown in Table 4. The results are summarized in Fig. 40 in terms of a ratio C_r defined as;

$$C_r = k_{h,crit}/(PHGA/g) \qquad (1)$$

where $k_{h,crit}$ is the critical horizontal seismic coefficient yielding a safety factor of unity. The value of PHGA was estimated as approximately 600 gal to 800 gal based on Fig. 5. For the RWs which actually failed, the values of $k_h = C_r \cdot (PHGA/g)$ as obtained would have under-estimated the correct values to be used in the aseismic design, because the critical PHGA at which the structures were about to fail should be equal to or smaller than the actual PHGA. The reverse is true for the RWs which did not fail.

In Fig. 40, the potential failure modes against external instability are also indicated. These failure modes were found consistent with the observed behaviour. The value of C_r against external instability for the GRS-RW at Tanata was 0.6 - 0.8, which was similar to those for the other conventional RWs excluding the cantilever-type RC RW at Shin-Nagata (CL2 in Fig. 4; see also Fig. 11). A very low value of C_r for the wall at Shin-Nagata would be due to the fact that the backfill was considerably sloped. Based on the results shown in Fig. 40 (excluding the wall at Shin-Nagata), the following conclusions could be drawn:

1) With respect to the external stability of the conventional RWs which had failed, the correction

Table 4 Design parameters for external seismic stability analysis of RWs (after Koseki et al., 1996).

Site		Sumiyoshi (Leaning type)	Ishiyagawa (Gravity type)	Ishiyagwa (Cantilever type)	Shin-Nagata (Cantilever type)	Tanata (GRS-RW)
Schematic diagram		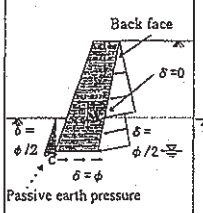	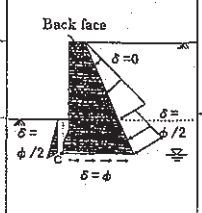	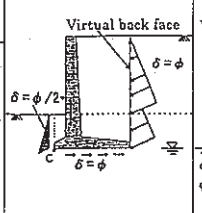	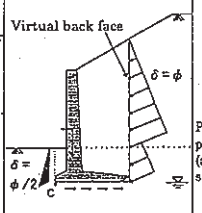	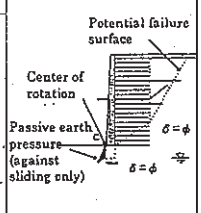
Concrete wall	γ (kN/m³)	23.2	22.7	22.5	23.2	24.5
Soil property used to evaluate earth pressure	γ (kN/m³)	18.1	17.5	17.5	16.1	16.7
	c (kN/m²)	0.0	0.0	0.0	0.0	0.0
	φ (°)	45	42	42	36	41
evaluate bearing capacity	c (kN/m²)	0.0	0.0	0.0	49.1	0.0
	φ (°)	41.8	35.8	35.8	0	33.4
Coefficient of bearing capacity	N_c	91	37	37	5.1	26
	N_γ	150	32	32	0	17
	N_q	82	24	24	1	15

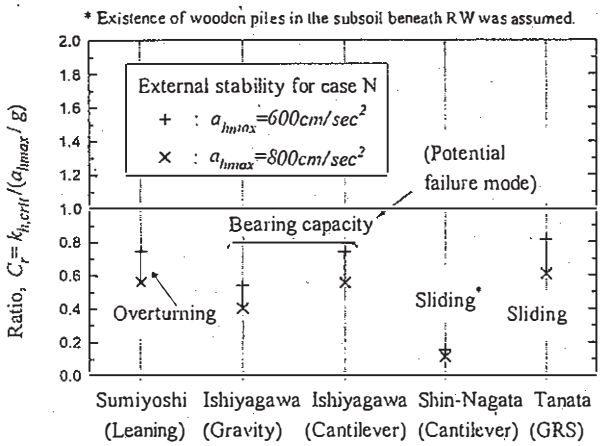

Fig. 40 Ratio of critical horizontal seismic coefficient to estimated PHGA for external stability of RWs (after Koseki et al., 1996).

factor C_r to be used to convert the design PHGA/g into the design seismic coefficient k_h in such that $k_h = C_r \cdot (PHGA/g)$ may be larger than 0.6 (but very likely smaller than 1.0).

2) For the GRS-RW at Tanata, the above correction factor for external instability may be smaller than that for the conventional RWs, considering the fact that the GRS-RW was only slightly damaged and has been reused while the other conventional RWs had to be removed for reconstruction.

3)As a whole, when the same pseudo-static seismic stability analysis method is used for both conventional RWs and GRS-RWs, the design would become more conservative for GRS-RWs.

In the current design procedure for the GRS-RW as employed in the aforementioned analysis, the safety factor against overturning is defined as:

$$F_s = \left\{ \frac{M_T + M_{WW} + M_{PV}}{M_{PH} + M_{WH}} \right\}_{min} \quad (2)$$

where M_T, M_{WW} and M_{PV} are the resisting moments due to, respectively, the tensile force of reinforcement acting at the back face of the facing, the self weight of facing, and the vertical components of both the earth pressure acting on the boundary between the front (F) and the back (B) wedges in the backfill ($P_{BF} \cdot \sin \phi_{BF}$ in Fig. 39) and the resultant earth pressure acting on the back face of the facing ($P_F \cdot \sin \phi_{FW} - P_{BF} \cdot \sin \phi_{BF}$ in Fig. 39). M_{PH} and M_{WH} are the overturning moments due to horizontal components of the earth pressure acting on the back face of the facing ($P_F \cdot \cos \phi_{FW}$ in Fig. 39) and the inertia force of the facing, respectively. This safety factor is principally based on the equilibrium of moments acting on the facing about its toe, but it is somewhat ambiguous because the vertical component of earth pressure acting on the boundary between F-wedge and B-wedge was expediently introduced in order to reflect the effect of the length of reinforcements (or the width of F-wedge).

On the other hand, when the equilibrium of moments about the facing toe acting on the facing and the F-wedge are considered, the safety factor can be defined alternatively as:

$$F_s = \left\{ \frac{M_{FT} + M_W}{M_P + M_R + M_H} \right\}_{min} \quad (3)$$

where M_{FT} and M_W are the resisting moments due to the tensile force of reinforcement mobilized at the boundary between F-wedge and B-wedge (PR in Fig. 39) and the bottom of F-wedge (OP in Fig. 39), and the self weight of both the facing and F-wedge, respectively. M_P, M_R and M_H are the overturning

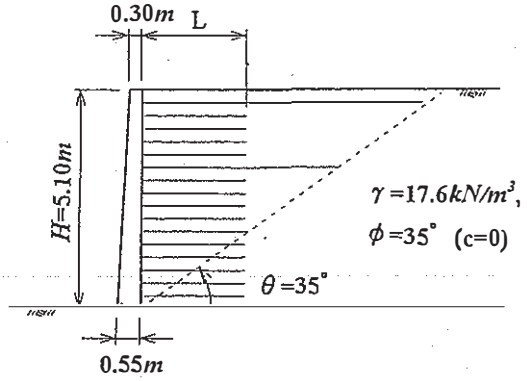

Fig. 41 A model GRS-RW having a FHR facing to estimate the effects of different stability analysis methods (after Horii et al., 1994).

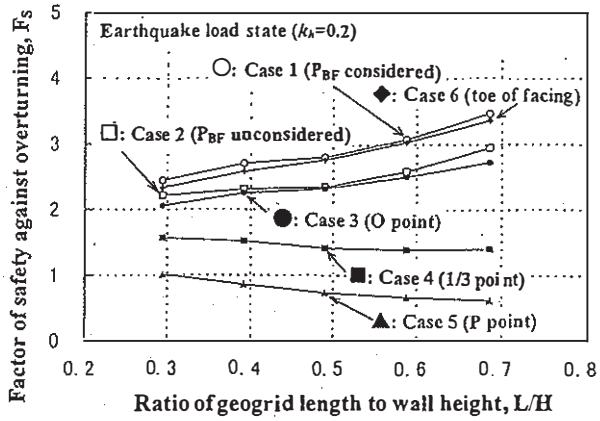

Fig. 42 Effects of different assumptions on the results obtained by two different seismic stability analysis methods for a model GRS-RW having FHR a facing.

moments due to, respectively, the earth pressure acting on the boundary between F-wedge and B-wedge (PBF in Fig. 39), the reaction force at the bottom of F-wedge (R_F in Fig. 39), and the inertia forces of both the facing and F-wedge.

The issues of differences in the safety factor between the two methods and the effects of the assumed location of the reaction force at the bottom of F-wedge or the facing have been discussed by Horii et al. (1994). Safety factors against overturning of a model wall shown Fig. 41 were evaluated under the following six conditions. Case 6 was added on by the authors.

Based on Eq.2

Case 1: Based on the equilibrium around its toe of moments acting on the facing about the facing toe, considering the effects of the vertical component of the earth pressure acting on the boundary between F-wedge and B-wedge in the backfill (P_{BF} in Fig. 39) (the current design procedure).

Case 2: The same equilibrium as above is considered, but not considering the effects of the component P_{BF}.

The alternative design procedure based on the equilibrium moments acting on the facing and the F-wedge about the facing toe (i.e., based on Eq.3)

Case 3: The reaction force at the bottom of F-wedge (R_F in Fig. 39) is assumed to act at point O in Fig. 39.

Case 4: The reaction force R_F is assumed to act at the one third point of the length OP from the point O.

Case 5: The reaction force R_F is assumed to act at point P in Fig. 39.

Case 6: The reaction force R_F is assumed to act at the facing toe (M_R is set to be zero).

Fig. 42 shows the change of safety factor against overturning by the change of the reinforcement length (L) normalized by the wall height (H) under seismic conditions when k_h = 0.2. The results can be summarized as follows;

1) In the alternative design procedure (Eq. 3), the results of cases 4 and 5 are not realistic, because the safety factor decreases as L/H increases. On the other hand, the stabilization effect by widening the reinforcement zone is reflected in the results of cases 3 and 6. The assumptions made in cases 3 and 6 may be acceptable when a FHR facing is employed with the subsoil having a sufficient bearing capacity against the somehow concentrated reaction force R_F at the facing base.

2) When based on Eq. 2, cases 1 and 2 yield similar results to cases 6 and 3, respectively. Therefore, the current design procedure considering the effect of the vertical component of the earth pressure acting on the boundary between F-wedge and B-wedge in the backfill (i.e. case 1) is judged to be reasonable as long as the momentary concentration of the reaction force at the facing toe due to the inertia force during an earthquake is allowed.

6.3 *Limitation of current seismic design*

Felio et al. (1990) reported that the safety factors of eight nailed slopes which did not fail during the 1989 Loma Prieta earthquake obtained based on the current limit equilibrium-based seismic stability analysis using the value of k_h equal to the estimated PHGA divided by g are considerably lower than unity. This was also the case with the nailed slopes during this earthquakes. They considered that the main reason is the hidden conservatism by neglecting effects of the bending and shear resistance of the reinforcement and the rigidity of facing.

The Tanata GRS-RW survived despite the use of k_h= 0.2 in the design, which is much lower than the PHGA/g at the site (about 0.6 - 0.8). Some hidden

conservatism may be one of the reasons. Other reasons may include a) under-estimated shear strength of backfill soil, and b) no consideration of passive earth pressure on the front face of the buried part of facing. The effects of H-shaped steel piles remaining behind the reinforced zone at the time of the earthquake would be small. Collins et al. (1992) also reported that during the 1989 Loma Prieta earthquake, two geogrid-reinforced RWs having wrapped-around wall face behaved very well for estimated PHGA/g of around 0.4, despite the design k_h was 0.1 - 0.2. Fukuda et al. (1994) also reported that a 6.7 m high geogrid-reinforced RW having a facing of steel wire mesh with a wall face slope of 1:0.3 in V:H, which was not aseismic-designed, was stable despite that the estimated PHGA was 310 gals.

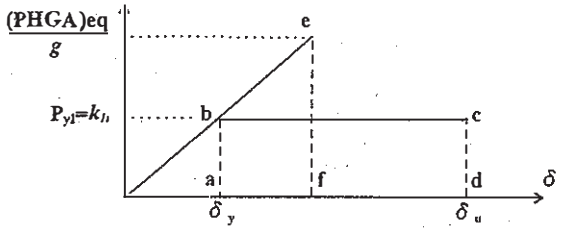

Fig. 43 Method to obtain the equivalent PHGA of a ductile structure.

It seems to the authors that the effect of the flexibility and ductility of reinforced soil RWs is yet another reasons. It is conceivable that as a RW becomes more flexible, the seismic earth pressure acting on its back face becomes smaller; and as the structure becomes more ductile, the design procedure where PHGA/g is used as k_h and the structure is judged to fail when the limit equilibrium is lost for the first time is too conservative. On the other hand, as the current seismic design procedures for soil structures are mostly limit equilibrium-based stability analysis, they cannot evaluate the deformation and displacement of soil structure caused by seismic loads, therefore they cannot evaluate the effects of flexibility and ductility on the seismic stability of a soil structure.

Effects of ductility: When some post-yield deformation without exhibiting complete collapse is allowed to occur, it could be judged that ductile structures C and E illustrated in Fig. 14 can sustain seismic load L exceeding the yield strength P_{yl}. In concrete engineering, the value of PHGA/g which is larger than P_{yl}, is obtained in such a way that the areas *abcd* and *abef* of the two load-deformation curves for linear elastic and ductile elasto-perfectly plastic materials are the same (Fig. 43). The above procedure is equivalent to the use of k_h

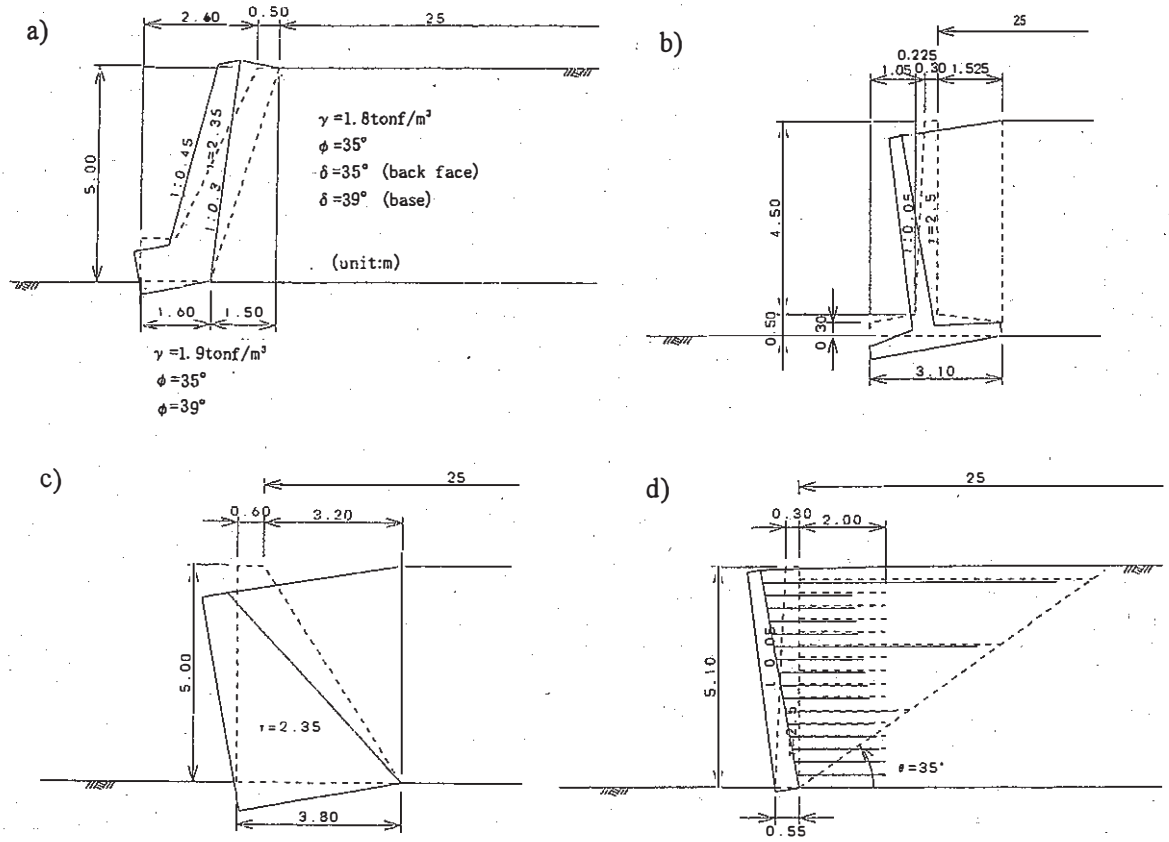

Fig. 44 Model RWs to evaluate the ductility in overturning failure.

smaller than PHGA/g (= L) in the limit equilibrium-based stability analysis. According to this methodology, the design k_h value for ductile soil structures could be set to be smaller than that for brittle soil structures.

Although in a very approximated way, one aspect of the structural ductility of RW could be evaluated by the rate of decrease in the safety factor for overturning with the increase in the overall overturning displacement as shown in Fig. 44. It was assumed in this analysis that the three conventional types of RWs overturn about the heel of the base, while the GRS-RW about the heel of the facing base. The backfill was assumed not to move, while the space produced by the displacement of the wall was filled up by additional soil. It was assumed that the bearing capacity failure and wall structure failure do not take place. Fig. 45 shows the reduction rate of safety factor for overturning when k_h= 0.2, plotted against the rotational angle θ of the wall. F_{s0} and F_s mean the safety factors before and after the occurrence of overturning. It is seen that the safety factor at seismic conditions (with k_h=0.2) decreases as the wall overturns, and the reduction rate is larger, following the order: the leaning type RW, gravity type RW, inverted T-shaped RC RW and GRS-RW. As the area between each curve and the horizontal axis becomes larger, the RW could be considered to be more ductile.

Effects of flexibility: It may be needed to classify RWs into dynamically rigid and flexible RWs and intermediate ones. "Dynamically rigid RWs" could be defined as those of which the dynamic displacement is much smaller than that of the backfill, and therefore the seismic earth pressure becomes larger than that at static states. The most conventional type soil RWs (i.e., leaning type and gravity type unreinforced concrete RWs and cantilever and inverted T-shaped RC RWs) which are stable during earthquakes are categorized as "rigid RWs". On the other hand, "dynamically flexible RWs" could be defined as those of which the displacement is similar to, or larger than, that of the backfill, and the seismic earth pressure is not larger, or smaller, than that at static states. Reinforced soil RWs may be categorized as "flexible RWs" or "intermediate ones".

Rigid walls should be designed to displace smaller than the backfill when subjected to seismic loads. The seismic earth pressure is evaluated usually by the Mononobe-Okabe method. Against the seismic earth pressure and the gravitational and inertia force applied to the wall structure, it is evaluated whether the wall structure, the bearing capacity of subsoil (or piles when used) and the shear strength at the interface between the wall base and the subsoil are

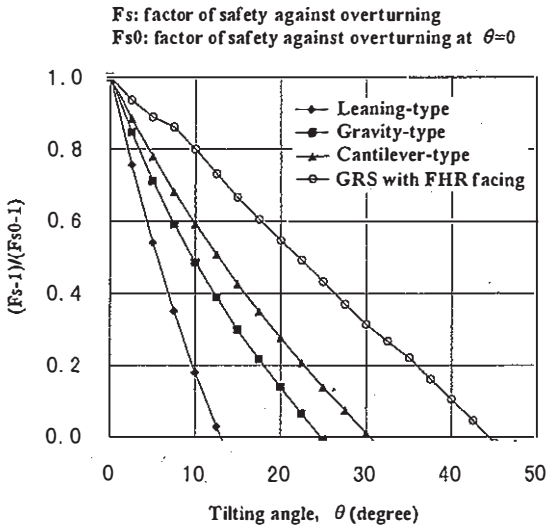

Fig. 45 Change in the safety factor due to overturning evaluated by the limit equilibrium pseudo-static method (k_h= 0.2).

all large enough, and whether the wall does not overturn. The deformation of the wall by seismic force is usually not examined.

In the current design methodologies, reinforced soil RWs are treated as rigid RWs. To the authors, it would be more reasonable to consider reinforced soil RWs as "flexible RWs" or "intermediate ones". In that case, the design seismic earth pressure could be made smaller than that for rigid RWs. However, in the following two types of analysis, it should be ensured that a given reinforced soil RW displaces and deforms in a ductile manner as "structure E", behaving as a wide flexible monolith;

1) the overall stability analysis for overturning and sliding at the base as that for rigid RWs; and
2) the internal deformation of the reinforced zone, including the issue of internal stability,

6.4 *Deformation of reinforced backfill as flexible RWs*

In case reinforced soil RWs are designed as "flexible RWs" or "intermediate ones", the following three types of internal deformation of the reinforced backfill should be evaluated (Fig. 46):

a) shear deformation along the potential failure plane;
b) simple shear deformation along horizontal planes; and
c) deformation due to overturning moment.

a) The horizontal outward seismic loads increase the disturbing shear stress τ_w acting along the potential failure plane (Fig. 46a). In an unreinforced backfill,

a) shear deformation along potential failure plane

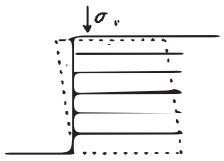

b) simple shear deformation along horizontal planes

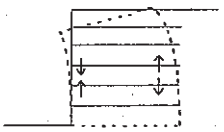

c) deformation due to overturning moment

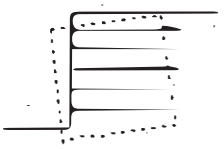

d) overturning due to deformation of subsoil layer

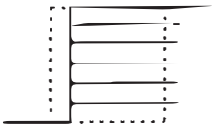

e) sliding at the boundary of reinforced zone and subsoil layer

Fig. 46 Different modes of deformation and displacements of GRS-RWs subjected to seismic loads.

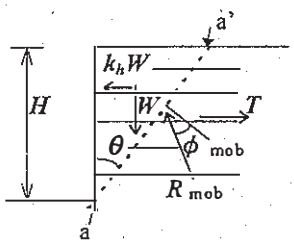

$W=(\gamma \cdot H^2 \cdot \tan\theta)/2$

k_h: horizontal seismic coefficient

H: wall height

T: total reinforcement force

Fig. 47 Simplified force equilibrium in reinforced soil RWs.

the normal stress σ_n acting on the potential failure surface decreases at the same time, which leads to a reduction in the soil shear strength $\tau_f = \sigma_n \cdot \tan\phi$. In a reinforced backfill, tensile force induced in the reinforcement resists directly against the shear stress τ_w and restrains the reduction in σ_n. This mechanism can be explained also by using a simple model shown in Fig. 47. For a backfill of cohesionless soil, the local safety factor $(F_s)_{rf}$ along a given plane a-a' in the direction at the angle θ from the vertical is defined as:

$$(F_s)_{rf} = \tan\phi / \tan\phi_{mob} \qquad (4)$$

where ϕ and ϕ_{mob} are the angle of internal friction (peak shear strength) and the mobilized angle of friction, referring to the mobilized reaction force R_{mob} acting on the plane. From the force equilibrium among the weight of the active zone W, the outward horizontal seismic force $k_h \cdot W$ and the total reinforcement force T, it follows:

$$(F_s)_{rf} = \tan\phi \cdot \frac{T/W + \tan\theta - k_h}{1 - (T/W)\cdot\tan\theta + k_h \cdot \tan\theta} \qquad (5)$$

The safety factor increases as T increases. The safety factor when the backfill is not reinforced is:

$$(F_s)_{unrf} = \tan\phi \cdot \frac{\tan\theta - k_h}{1 + k_h \cdot \tan\theta} \qquad (6)$$

The ratio between the above two is;

$$\frac{(F_s)_{rf}}{(F_s)_{unrf}} = \frac{1 + (T/W)/(\tan\theta - k_h)}{1 - \{(T/W)\cdot\tan\theta\}/(1 + k_h \cdot \tan\theta)} \qquad (7)$$

Since the value of θ at which the value of Fs becomes the minimum is around $45° - \phi/2$ and T/W is much smaller than 1.0, the ratio for the critical plane increases with k_h. That is, with the increase in k_h, a reinforced RW becomes more stable relative to the corresponding unreinforced RW. This means that the advantages of reinforced RWs become more apparent in the aseismic-design. It is also the case with the relative stability between unreinforced and reinforced slopes.

Note also that the use of a FHR facing is effective to restrain the development of a failure plane which intersects the facing at intermediate heights.

b) In case the deformation of reinforced backfill is restrained to simple shear deformation along horizontal planes, the stress condition becomes uniform along each horizontal plane and the length of each horizontal plane is kept constant. To realize these conditions, the following two requirements

should be satisfied:

i) Relatively inextensible reinforcement is arranged horizontal to achieve zero or nearly zero normal strains in the horizontal directions.

ii) A facing with sufficient axial rigidity while having sufficient vertical bearing capacity at the facing base is arranged to transmit the axial force so that the upward shear stress τ_{hv} can be activated along the vertical face of the backfill in contact with the back face of the facing (Fig. 48). Without this complementary shear stress τ_{hv}, the shear stress τ_{vh} cannot be exerted on the horizontal planes. As the back face of the reinforced zone is inside a soil mass, the complementary shear stress τ_{hv} is exerted automatically on this plane.

In addition, the shear strength $(\tau_{vh})_{max}=(\tau_{hv})_{max}$ is controlled by the vertical and horizontal stresses σ_v and σ_h as;

$$(\tau_{vh})_{max}=(\tau_{hv})_{max}= (1/2)\cdot\{(\sigma_v+\sigma_h)^2\cdot\sin^2\phi-(\sigma_v-\sigma_h)^2\}^{1/2} \quad (8)$$

It is seen from the above equation that under a constant σ_v, the shear strength $(\tau_{vh})_{max}$ (and shear rigidity) increases as σ_h increases, resulting in smaller shear deformation of the reinforced backfill. Therefore, the simple shear deformation becomes smaller by maintaining larger horizontal stress σ_h. The use of a FHR facing to which reinforcement layers are connected contributes to the above, although it is in an indirect way. It is to be noted that even under the same seismic conditions, the stresses in the FHR facing of GRS-RW become much smaller than those in the cantilever-type RC RWs, since the FHR facing is supported at many elevations by reinforcement layers, behaving as a continuous vertical beam with a rather short span (Tatsuoka, 1993).

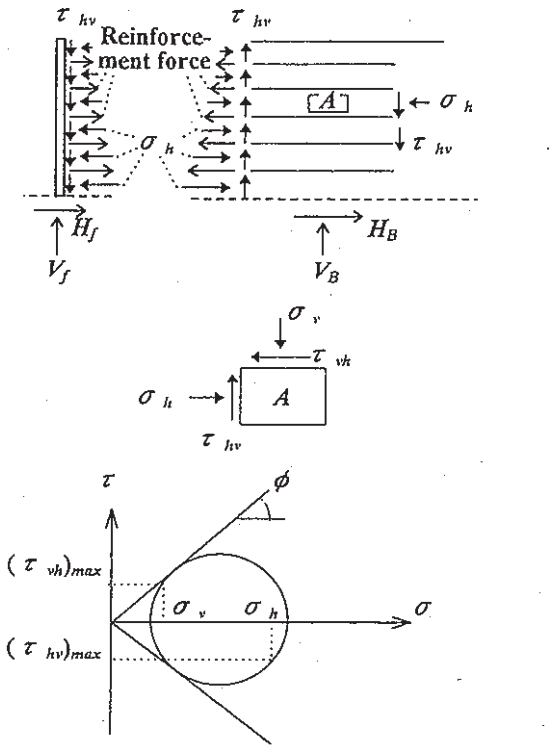

Fig. 48 Stress condition on the back of a full-height rigid facing.

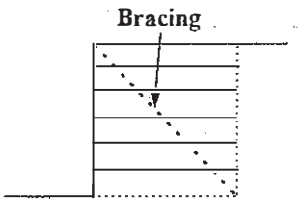

Fig. 49 Bracing in a reinforced soil RW.

Moreover, as the shear deformation of the reinforced backfill increases, a constant length of facing results in a reduction in the height of the reinforced backfill zone adjacent to the facing, while the height of the backfill trends to increase due to dilatancy effects. Then, the vertical stress σ_v may increase in that zone. This factor would be an additional contribution of a FHR facing. It is noted, however, that this behaviour is realized only after large deformation.

Note that all the above-mentioned possible contributions of a FHR facing to the seismic stability of GRS-RW are indirect. The use of a bracing as shown in Fig. 49 would be much more direct and efficient. Nevertheless, it would not be very practical in actual construction. Indeed, the low capability for resisting against simple shear deformation is one of the largest problems in the seismic stability of reinforced soil RWs. This situation is similar to that of elevated RC frame structures (Fig. 1a).

When the horizontal displacement is uniform throughout the reinforced and unreinforced zones of an embankment, the amount of simple shear deformation is independent of the aspect ratio of the reinforced zone, or the reinforcement length. In case the displacement decreases away from the wall face, then the use of longer reinforcement, particularly at higher levels, would be effective to restrain the simple shear deformation (Fig. 50).

c) When using a FHR facing supported by a subsoil having sufficiently large bearing capacity, the overturning moment due to seismic force $k_h \cdot W$ and some additional seismic earth pressure exerting at the

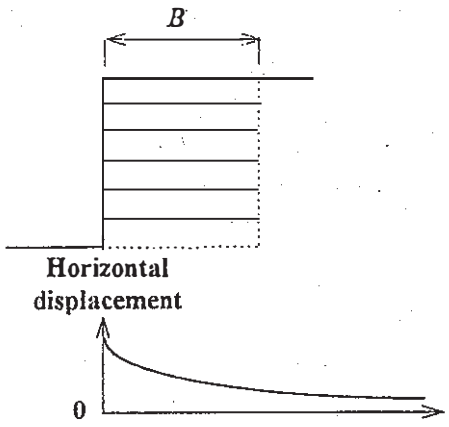

Fig. 50 A possible distribution of outward lateral displacement in reinforced soil RWs.

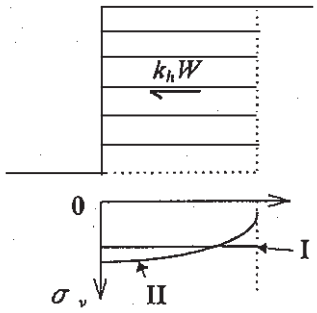

I: before earthquake

II: during earthquake

Fig. 51 Change in the vertical pressure at the base of reinforced soil RW without a FHR facing.

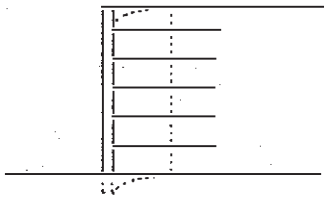

Fig. 52 Vertical shear deformation near the FHR facing due to the loss of bearing capacity of the subsoil

back face of the reinforced zone is resisted by the shear stress τ_{hv} acting upwards along the front face of the backfill (Fig. 48). The vertical load V_f at the facing base is the weight of the facing plus the integration of τ_{hv}. With this, the overall overturning of the reinforced backfill is restrained. Without a FHR facing, on the other hand, the vertical stress σ_v within and at the base of the reinforced backfill increases near the wall face and decreases near the back of the reinforced zone (see Fig. 51). This results in the deformation of the backfill as shown in Fig. 46c and the deformation of the subsoil as shown in Fig. 46d, both of which increase the overall tilting of the reinforced backfill.

Although the bearing capacity at the base for a FHR facing is important, it could be still secondary for the ultimate failure of a reinforced soil RW as was observed in a large model during shaking table tests (Fig. 26). When the bearing capacity at the facing base is lost, the flexible reinforced backfill soil would exhibit vertical shear deformation to accommodate it as illustrated in Fig. 52, while increasing the horizontal shear deformation and overall overturning deformation. On the other hand, for conventional RWs (e.g., gravity type unreinforced concrete RWs and cantilever RC RWs) without piles, stress tends to be concentrated at and near the toe of the base as the wall tends to overturn, which may lead to the loss of the vertical bearing capacity, resulting in the overall overturning displacement. To avoid this behaviour, most of recent conventional type RC RWs are supported with piles except when constructed on a very firm subsoil. This arrangement makes the conventional RWs less cost-effective than reinforced soil RWs.

6.5 *Reinforced soil bridge abutment subjected to seismic loads on the crest*

Bridge abutments should be able to support a RC block on which a bridge girder is directly placed, exhibiting vertical and horizontal displacements that are within the allowable limits. This was also one of the major issues when designing the three GRS bridge abutments having FHR facings shown in Fig. 53 (Tatsuoka et al., 1996c). Soon after the wall completion, cyclic lateral loads were applied to the front face of RC block denoted by the letter A in Fig. 53. The width of the reinforced bridge abutment is about 9 m. As seen from Fig. 54, for a maximum load of 98 kN (10 tonf), the displacement at the facing having a width of about 9 m was very small. Importantly, the FHR facing displaced not only near the top but near the bottom, which indicates that the FHR facing as a whole resisted against the lateral load. This is another important possible contribution of FHR facing to the seismic stability of reinforced soil RW. The lateral load in this test was limited to 98 kN (10 tonf) to avoid any possible damage to the structure. In similar lateral loading tests, a lateral load of 196 kN (20 tonf) was applied to a 3 m-wide test section of a 5 m-high full-scale model GRS-RW having a FHR facing (Tamura et al., 1994, Tateyama et al., 1994). The wall and facing did not show any sign of failure.

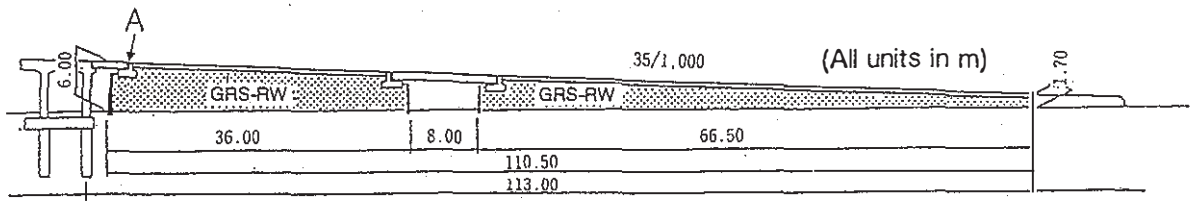

Fig. 53 Side view of GRS-RW and GRS bridge abutments for Seibu Line, at Nerima; the letter A shows the location of the lateral loading test (Tatsuoka et al., 1996c).

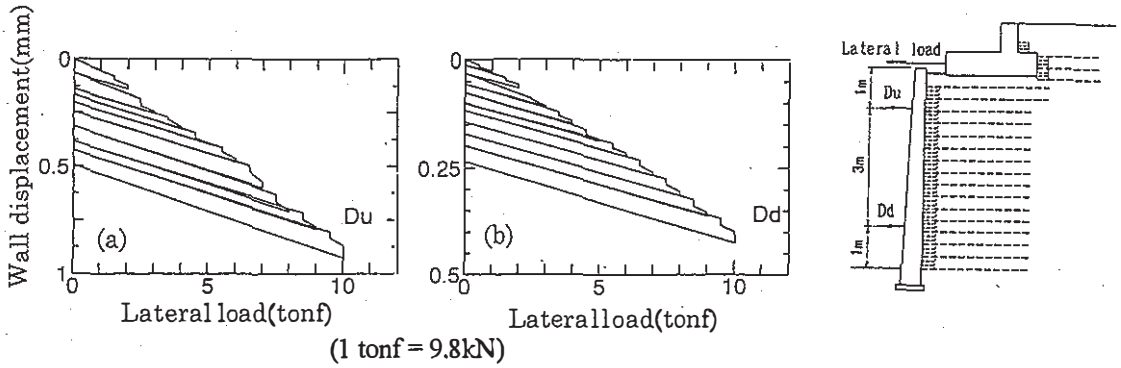

Fig. 54 Results of cyclic lateral loading test on a GRS bridge abutment for Seibu Line.

6.6 *Possible future trends of aseismic design*

So far, for most slopes, whether reinforced or not, the seismic stability is not evaluated in ordinary design procedures. It is also the case with usual highway and railway embankments having a height lower than, say, 5 m. As discussed earlier, reinforced soil structures become more stable relative to unreinforced ones as seismic loads increase. Therefore, if seismic stability analysis becomes a standard design procedure, more often than not reinforced soil structures will be adopted.

After this earthquake, the following two stage aseismic-design procedure has been accepted by Japanese civil engineers to be applied to civil engineering structures to a greater extent than before the earthquake. That is, the following two level seismic loads are used, associated with each respective objective of aseismic design (JSCE, 1996):
1) Level one seismic load, which is expected to strike the structure once or twice during its service life. Structures should not be damaged under Level one earthquake motions.
2) Level two seismic load, which is very rare in its occurrence but has a very high impact in its intensity. It includes ground motions generated in epicentral regions of large scale inter-plate earthquakes and those generated in near-field area of causative inter-plate faults. Structures may be damaged under Level two earthquake motions, where design should be practiced to control their damage processes. It is considered that the seismic loads in the most severely shaken areas shown in Fig. 4 are equivalent to Level two seismic load. It is apparent that if the above procedure is to be adopted also for soil structures, the following two problems should be solved:

1) When the pseudo-static seismic stability method is used, the ratio "k_h/(design PHGA/g)" should be less than unity. Then, what value should be adopted for the ratio ? The ductility should be taken into account in a proper way when designed for Level two seismic load. Then, how could the ductility be defined ? And how could the ductility be reflected in the ratio "k_h/(the design PHGA/g)" ?
2) The dynamic flexibility of structure should be defined properly. Then, what would be a proper method to evaluate the effects of flexibility on the seismic earth pressure acting on the back of a soil retaining structure ?

Even if sophisticated seismic design methods considering the above two factor are developed and can be applied to reinforced soil RWs, it is not likely that they are applied equally to unreinforced and reinforced slopes. This is because the soil conditions in natural slopes are much more difficult to identify and much more heterogeneous than in backfills. A much simpler but rational method need to be developed.

6.7 *Seismic stability of PL/PS reinforced soil*

One of the advantages of reinforced soil structures in reducing the effects of seismic loads may be its flexibility. However, if it is too flexible, the deformation may exceed the allowable limit. The preloading and prestressing technique has been proposed originally to increase the vertical stiffness of reinforced soil structures (Tatsuoka et al., 1996a,b,c, Uchimura et al., 1996). As shown in Fig. 55, a vertical load is applied as preload to a reinforced backfill by using a pair of reaction blocks and a set of tie rods (or by using a top reaction block and a set of tie rods with the bottom ends anchored in the subsoil). After some creep deformation of the backfill has occurred at the preloading stage, the load is reduced to a lower level, which is then maintained as prestress. When sufficient amount of prestress has survived, a high pressure level (thereby high stiffness) is maintained in the backfill, which results in smaller deformation when subjected to seismic loads. Furthermore, when a PL/PS reinforced backfill is to be subjected to large shear deformation, it would exhibit highly ductile behaviour. This is because, as the length of the tie rods are maintained nearly constant, the height of backfill is forced to reduce with shear deformation, which results in an increase in the pressure level and thereby the increase in the stiffness. This mechanism will be enhanced if the backfill is well compacted to induce considerable dilative characteristics upon shear deformation. This behaviour is similar to that of saturated dense sand subjected to shear deformation under undrained conditions.

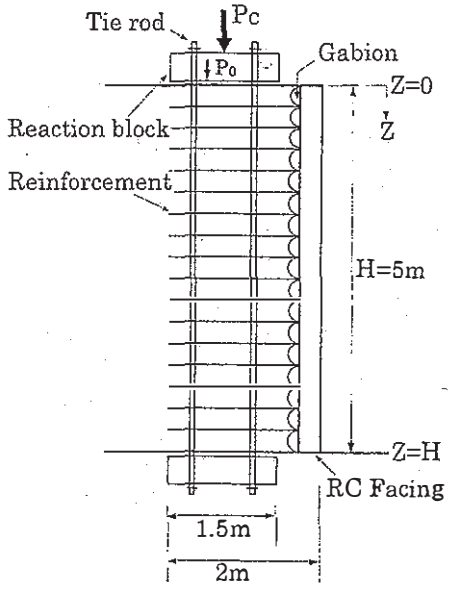

Fig. 55 Schematic diagram of PL/PS geosynthetic-reinforced soil RW (Tatsuoka et al., 1996a, b and c, Uchimura et al., 1996).

7. REMEDY WORKS AND RECONSTRUCTIONS BY SOIL REINFORCEMENT TECHNIQUES

After the earthquake, a large amount of remedial and preventive work of soil structures (i.e., sloped embankments, RWs and slopes) was performed by means of a variety of soil reinforcement techniques. This is another good evidence how these techniques have been accepted by civil engineers because of their cost-effectiveness and their performance.

7.1 *GRS-RWs with FHR facings*

Most of the embankment slopes and conventional type RWs for railways that were damaged seriously were replaced with GRS-RWs with FHR facings. Typical cases are shown in Figs. 8b, 9b, 10b and 11b. The total length of the walls constructed for remedial work is 1.1 km with the wall height ranging from 2 m to 5 m.

7.2 *Terre Armee walls*

Immediately to the south of JR Nada Station (see Fig. 4), the south slope of a road had been retained by RC RWs for a total length of 260 m at two elevations (see Fig. 56a) (Kobayashi and Ohtani, 1996). These RC RWs and the backfill moved significantly. The walls were replaced by Terre Armee walls, which were designed by using k_h= 0.15 (see Fig. 56b). The backfill soil consisted of 76 % gravel, 15 % sand and 9 % fines.

7.3 *Large diameter nailing in embankment slopes*

Many embankment slopes for railways were reinforced by using 40 cm-diameter nails as shown in Fig. 57. Each nail consists of a tendon of fiber-reinforced plastic (FRP) with a diameter of 37 mm (Tateyama et al., 1992). Each nail is produced by auguring the embankment slope, and then extruding the auguring device, supplying cement slurry from the blades at the end of the augur rod and mixing it with the surrounding soil while leaving the FRP rod at the center of the cylindrical zone of augured soil.

To construct a vertical RW, first vertical cement slurry-mixed soil columns are produced in the slope as pre-propping. Then, while excavating the slope, these large diameter nails are installed in stages. Finally, a thin RC facing is cast-in-place on the excavated slope. This method has been used to excavate the railway embankment slopes while allowing trains to run on the embankment for a total

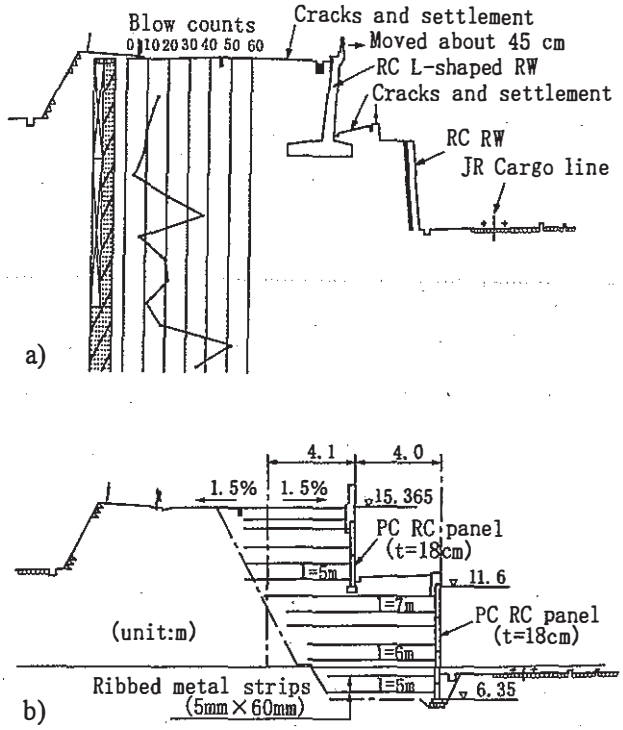

Fig. 56 a) Damaged RC cantilever RW for road embankment and b) Terre Armee wall by reconstruction, south of Nada Station, JR Kobe Line (Kobayashi and Ohtani, 1996).

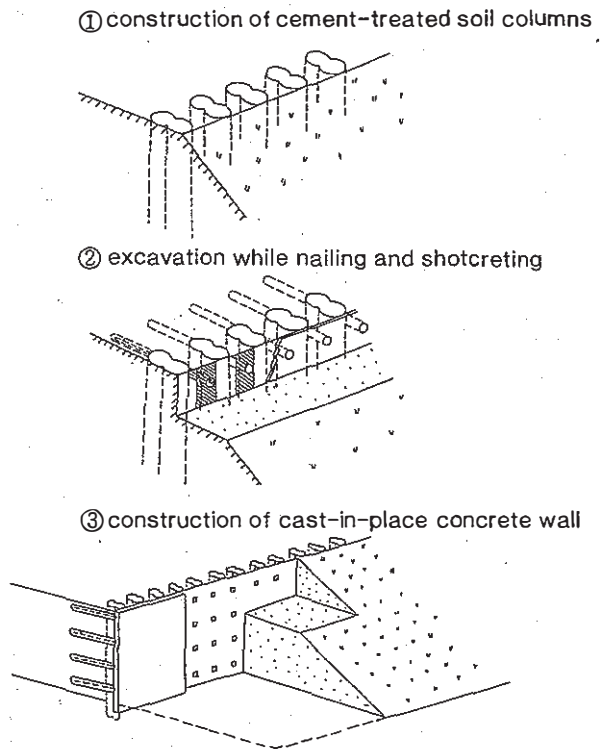

Fig. 57 Illustration of the large diameter nailing technique for vertical cutting of embankment slope (Tateyama et al., 1992, Tatsuoka, 1993).

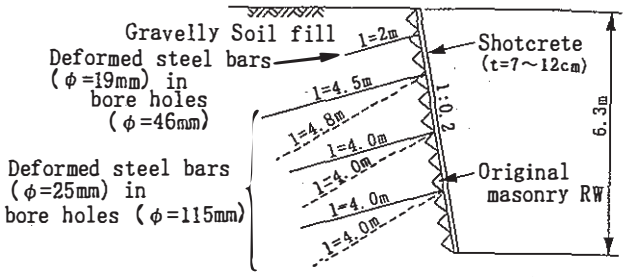

Fig. 58 Typical preventive work of slope by the root piling technique (Kobayashi and Ohtani, 1996).

length of more than 2 km. A completed structure is a sort of reinforced soil RW with a FHR facing. As the remedial work after this earthquake, damaged RWs and embankment slopes for railways were reconstructed by this technique for a total length of 530 m with the wall height ranging up to 6 m (Fig. 10c).

7.4 *Root-piling in natural slopes*

More than forty slopes were remedied or reinforced preventively for possible earthquakes in the future by using the root piling technique from either the crest of slope or the slope face or wall face. The case shown in Fig. 58 is typical of the walls stabilized by root piling from the wall face (Kobayashi and Ohtani, 1996). This masonry wall, located in Chuo-ku, Kobe City, was moved by the earthquake, while cracks appeared on the wall face and on the ground surface on the crest. The backfill soil was a sand gravel showing a SPT blow count of about five.

8 CONCLUSIONS

Different types of soil retaining walls (RWs) located in the severely shaken areas during the 1995 Hyogoken-Nanbu earthquake performed differently. In general, older RWs were damaged more seriously, while masonry, leaning-type and gravity-type unreinforced concrete RWs showed a very low stability against the strong seismic shaking. In addition, many cantilever-type or inverted T-shaped RC RWs, mostly without piles, performed poorly.

A great number of RC columns and piers collapsed by shear failure in a brittle manner.

In comparison with the above, a number of geogrid- or metal-reinforced soil RWs performed very well. In particular, the geogrid-reinforced soil RWs with FHR facings that were constructed in 1992 at Tanata did not collapse despite the fact that the site was located in one of the most severely shaken and

seriously damaged areas. Based on these experiences, many damaged embankment slopes and conventional RWs were replaced with GRS-RWs with FHR facings.

A number of natural slopes which had been stabilized by the nailing and root piling techniques also performed very well. A large amount of natural slopes and backfills of RWs were reinforced by these techniques after the earthquake.

For better understanding of the seismic behaviour and for developing more rational seismic design methodology of soil structures, the effects of flexibility on the seismic earth pressure and the effects of ductility on the design seismic coefficient to be used in limit equilibrium-based pseudo-static stability analysis should be studied. The internal deformation of reinforced backfill when subject to seismic loads and the effects of the facing rigidity and reinforcement length should also be studied.

It is not easy to restrain the simple shear deformation of reinforced soil RWs because of the lack of a bracing component, as in elevated RC frame structures. Preloading and prestressing the reinforced backfill may be effective to prevent such deformation.

ACKNOWLEDGMENTS

The authors wish to thank Messrs. Miyatake,H. and Tsutsumi,T. of Public Works Research Institute, Ministry of Construction, Horii,K. of Chuo Kaihatsu Corporation, Ohtani,Y. of Hirose Co.,Ltd., Torii,T. of Construction Project Consultants Inc., and Shintani,H. of Mitsubishi Yuka Industrial Products Co.,Ltd. and Mr. Sato,T., Ms. Torimitsu,M. and Dr. Kodaka,T. of IIS, Univ. of Tokyo for their assistance in the preparation of this paper. They also appreciate a careful review of the manuscript by Prof. Wu, J.T.H, the University of Colorado at Denver.

REFERENCES

Chuo Kaihatsu Corp. 1995. Report of damage investigation for the Great Hanshin earthquake, No.2- damage ratio investigation and geology and ground conditions. (in Japanese)

Collins,J.G., Chouery-Curtis,V.E. and Berg,R.R. 1992. Field observation of reinforced soil structures under seismic loading, Int. Symp. Earth Reinforcement Practice (Ochiai et al., eds), IS Kyushu '92, Balkema, Vol.1, pp.223-228.

Felio,G.Y., Vucetic,M., Hudson,M. Barar,P. and Chapman,R. 1990. Performance of soil nailed walls during the October 17, 1989 Loma Prieta earthquake, 43rd Canadian Geotechnical Conference, Quebec, pp.165-173.

Fujii,T., Sueoka,T., Muramatsu,M., Mega,M. and Ohtani,M. 1996. Behaviour of soil nailed walls and root pile structures caused by the 1995 Hyogoken-Nanbu earthquake, Symposium on Reinforcement of Natural Slopes, the Japanese Geotechnical Society, pp.1-191. (in Japanese)

Fukuda,N., Tajiri,N., Yamanouchi,T., Sakai,N. and Shintani,H. 1994. Applicability of seismic design methods to geogrid reinforced embankment, Proc. 4th Int. Conf. on Geotextiles, Geomembranes and Related Products, Singapore, pp.533-536.

Horii,K.,Kishida,H., Tateyama,M. and Tatsuoka,F. 1994. Computerized design method for geosynthetic-reinforced soil retaining walls for railway embankments, Recent Case Histories of Permanent Geosynthetic-Reinforced Soil Retaining Walls, Tatsuoka & Leshchinsky (eds.), Balkema, pp.205-218.

Japan Multiple Anchor Association (JMAA), 1995. Report on the behaviour of multiple-anchor-reinforced soil retaining walls during the Hyogoken-Nanbu earthquake. (in Japanese)

Japan Society of Civil Engineers, 1996. Proposal on earthquake resistance for civil engineering structures (Special Task Committee of Earthquake Resistance of Civil Engineering Structures), The 1995 Hyogoken-nanbu Earthquake -Investigation into Damage to Civil Engineering Structures-, Committee of Earthquake Engineering, Japan Society of Civil Engineers, pp.297-306.

Japan Terre Armee Association (JTAA), 1995. Report on the behaviour of Terre Armee walls during the Hyogoken-Nanbu earthquake. (in Japanese)

Kobayashi,K and Ohtani,Y. 1996. Damage and restoration of reinforced earth structures in the 1995 Hyogoken-Nambu Earthquake, The Foundation Engineering & Equipment, Vol.24, No.10. (in Japanese)

Koseki,J., Tateyama,M., Tatsuoka,F. and Horii,K. 1996. Back analyses of soil retaining walls for railway embankments damaged by the 1995 Hyogoken-Nanbu Earthquake, The 1995 Hyogoken-nanbu Earthquake -Investigation into Damage to Civil Engineering Structures-, Committee of Earthquake Engineering, Japan Society of Civil Engineers, pp.101-114.

Matsui,T., Kobayashi,K., Kumada,T. and Ohtani,Y. 1996. Damage of reinforced earth structures by steel reinforcements in the 1995 Hyogoken-Nanbu earthquake, Tsuchi-to-Kiso, Vol.44, No.2, pp.76-78. (in Japanese)

Ministry of Transport, 1992. Design standards for railway structures - soil structures-. (in Japanese)

Mitsubishi Yuka Industrial Products Co.,Ltd., 1995. Survey report on the damage induced by the 1995 Hyogoken-Nanbu earthquake. (in Japanese)

Murata,O., Tateyama,M. and Tatsuoka,F. 1994. Shaking table tests on a large geosynthetic-reinforced soil retaining wall model, Recent Case Histories of Permanent Geosynthetic-Reinforced Soil Retaining Walls, Tatsuoka & Leshchinsky (eds.), Balkema, pp.259-264.

Naemura,S. and Miyatake,H. 1995. Damage to earth structures for road facilities in the Hanshin-Awaji earthquake disaster, Technical information on geosynthetics, Vol.11, No.2, Japan Chapter of the Int. Geosynthetics Society, pp.3-8. (in Japanese).

Nishimura,J., Hirai,T., Iwasaki,K., Saitoh,Y., Morishima,M., Shintani,H., Yoshikawa,S. and Yamamoto,H. 1996. Earthquake resistance of geogrid-reinforced soil walls based on a study conducted following the southern Hyogo earthquake, Prof. Int. Symp. on Earth Reinforcement, IS Kyushu '96, Balkema Vol.1, pp.439-444.

Ohbayashi Corp., 1995. Preliminary report on the 1995 Southern Hyogo Prefecture Earthquake, Ohbayashi Corporation Technical Research Institute, p.16.

Research Committee on Reinforcement Technology for Natural Slopes, 1996. Activity report, Symposium on Reinforcement of Natural Slopes, Japanese Geotechnical Society, pp.1-191. (in Japanese)

Railway Technical Research Institute (RTRI), 1996. Reconnaissance report on damage of railway facilities in Hyogo-ken Nanbu earthquake, Special No.4, pp.56-62. (in Japanese)

Sassa,K., Fukuoka,H., Scarascia-Mugnozza,G. and Evans,S. 1996. Earthquake-induced-landslides: distribution, motion and mechanisms, Special Issue of Soils and Foundations on Geotechnical Aspects of the January 17 1995 Hyogoken-Nambu Earthquake, pp.53-64.

Sato,T. 1996. Estimation of peak acceleration in the severely damaged area during the 1995 Hyogo-ken Nanbu earthquake, The 1995 Hyogoken-Nanbu Earthquake -Investigation into Damage to Civil Engineering Structures-, Committee of Earthquake Engineering, Japan Society of Civil Engineers, pp.35-44.

Tamura,Y., Nakamura,K., Tateyama,M., Murata,O., Tatsuoka,F. and Nakaya,T. 1994. Full-scale lateral loading tests of column foundations in geotextile-reinforced soil retaining walls, Recent Case Histories of Permanent Geosynthetic-Reinforced Soil Retaining Walls, Tatsuoka & Leshchinsky (eds.), Balkema, pp.277-285.

Tateyama,M., Murata,O., Tamura,Y., Nakamura,K., Tatsuoka,F. and Nakaya,T. 1994. Lateral loading tests of columns on the facing of geotextile-reinforced soil retaining wall, Recent Case Histories of Permanent Geosynthetic-Reinforced Soil Retaining Walls, Tatsuoka & Leshchinsky (eds.), Balkema, pp.287-294.

Tateyama,O., Tarumi,H., Tamura,Y. and Tatsuoka, F. 1992. Permanent cut of an embankment slope by soil nailing allowing very small deformation, Earth Reinforcement Practice (Ochiai et al., eds), IS Kyushu, Balkema, Vol.1, pp.555-560.

Tatsuoka,F., Murata,O. and Tateyama,M. 1992. Permanent geosynthetic-reinforced soil retaining walls used for railway embankment in Japan, Geosynthetic-Reinforced Soil Retaining Walls, Wu (ed.), Balkema, pp.101-130.

Tatsuoka,F. 1993. Roles of facing rigidity in soil reinforcing, Keynote Lecture, Proc. Int. Sym. on Earth Reinforcement Practice, IS Kyushu '92, Balkema (Ochiai et al., eds), Vol. 2, pp.831-870.

Tatsuoka,F., Tateyama,M. and Koseki,J. 1996. Performance of soil retaining walls for railway embankments, Soils and Foundations, Special Issue of Soils and Foundations on Geotechnical Aspects of the January 17 1995 Hyogoken-Nambu Earthquake, pp.311-324.

Tatsuoka,F., Uchimura,T. and Tateyama,M. 1996a. Preloaded and prestressed reinforced soil, Soils and Foundations (accepted for publication)

Tatsuoka,F., Uchimura,T., Tateyama,M. and Muramoto,K. 1996b. Creep Deformation and Stress Relaxation in Preloaded/Prestressed Geosynthetic-Reinforced Soil Retaining Walls, Session "Measuring and Modeling Time-Dependent Soil Behavior", ASCE Washington Convention, pp.258-272.

Tatsuoka,F., Tateyama,M, Uchimura,T. and Koseki,J. 1996c. Geosynthetic-Reinforced Soil Retaining Walls as Important Permanent Structures, The 1996-1997 Mercer Lecture, Proc. of Euro-Geo, First European Geosynthetic Conference and Exhibition, Maastricht, the Netherlands, pp.3-24.

Tsukuda,C., Yamamoto,A. and Fukuda,N. 1996. Stability analysis of cut slope reinforced with steel bars at north area of Awaji Island during Hyogoken-Nambu earthquake, Symposium on Reinforcement of Natural Slopes, the Japanese Geotechnical Society, pp.295-298. (in Japanese).

Uchimura,T., Tatsuoka,F., Sato,T., Tateyama,M. and Tamura,Y. 1996. Performance of preloaded and prestressed geosynthetic-reinforced soil, Proc. Int. Symp. on Earth Reinforcement, Fukuoka, Balkema (Ochiai et al., eds), Vol. 1, pp.537-542.